E-ISSN: 3062-2107
Volume 2
Issue 1
2026

CALCULATION

The Calculation Journal publishes original results in science, engineering and social sciences in which intensive mathematical methods are used.

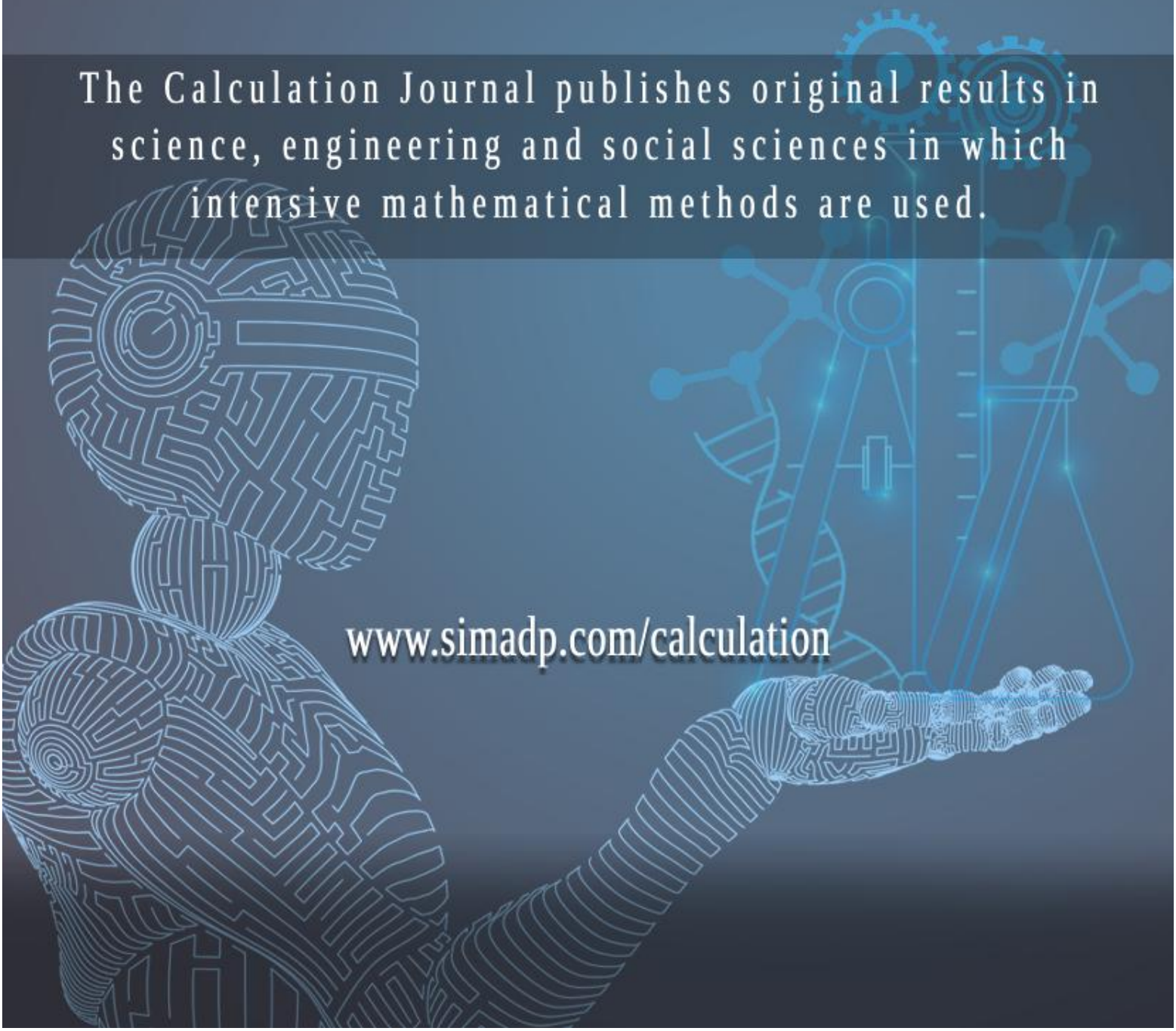

www.simadp.com/calculation

VOLUME 2 ISSUE 1
E-ISSN: 3062-2107

January 2026
www.simadp.com/calculation

The Journal CALCULATION

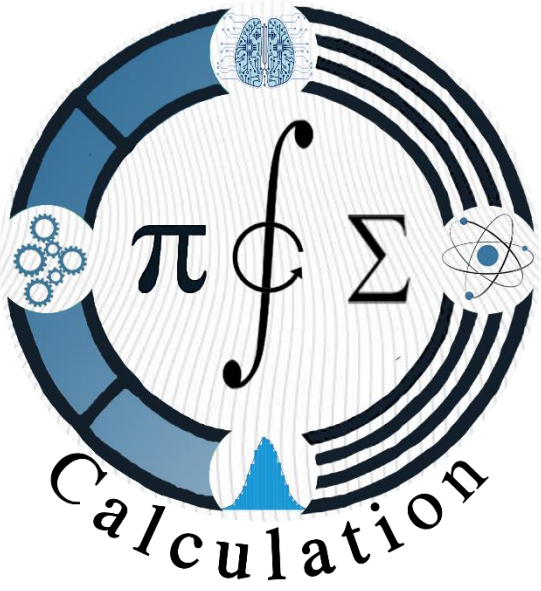

Editor-in-Chief

Bayram Sahin
Department of Mathematics, Faculty of Science, Ege University, Izmir, Türkiye
calculationjournal@gmail.com

VOLUME 2 ISSUE 1
E-ISSN: 3062-2107

January 2026
www.simadp.com/calculation

Contents

CALCULATION

Volume ***2****, Issue* ***1****, 2026, Pages:****1–1***

E-ISSN: 3062–2107

www.simadp.com/calculation

EDITORIAL

BAYRAM ŞAHİN *

With the publication of Volume 2, Issue 1, CALCULATION marks the completion of its first year as an international, peer-reviewed scientific journal. This milestone reflects the growing engagement of the scientific community with the journal's scope, standards, and editorial vision.

CALCULATION is dedicated to publishing original research in mathematics and in scientific disciplines where mathematical methods play a central role, including computer science, physics, chemistry, statistics, and engineering sciences. The articles published in the first volume have covered both theoretical and applied studies, highlighting the importance of interdisciplinary approaches and methodological innovation. We are also pleased to note that CALCULATION is indexed in the ROAD (Directory of Open Access Scholarly Resources), reinforcing its visibility and accessibility within the global research community.

As CALCULATION enters its second volume, we reaffirm our commitment to advancing scientific knowledge by providing a reliable and inclusive platform for researchers worldwide. We sincerely thank our authors, reviewers, and editors for their valuable contributions during the journal's first year and look forward to continued scholarly collaboration.

In the second year of our journal CALCULATION, we welcome Professor Arif Salimov as our new editor. Professor Salimov is the Head of the Department of Algebra and Geometry at the Faculty of Mathematics and Mechanics, Baku State University, and a full professor specializing in differential geometry. Having also served as a professor at Atatürk University in Türkiye, Professor Salimov has contributed to the scientific world by graduating numerous doctoral students. He has received Turkic World Science Awards, including the Khwarizmi Mathematics Prize from Baku State University. He is the author of over 100 articles and 2 monographs.

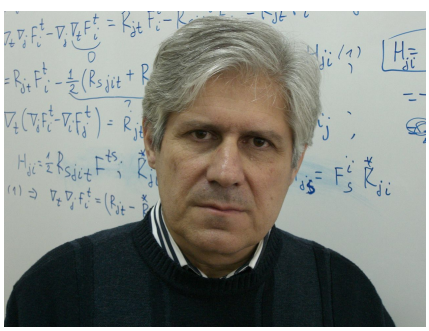

Arif Salimov

We are confident that Professor Salimov will make significant contributions to CALCULATION as its editor, and we welcome him once again.

* Editor-in-Chief

CALCULATION

Volume ***2****, Issue* ***1****, 2026, Pages:****2–11***

E-ISSN: 3062–2107

www.simadp.com/calculation

ON THE STRUCTURE OF ALMOST RICCI-BOURGUIGNON SOLITONS IN LORENTZIAN PARA-KENMOTSU GEOMETRY

SWAPNA SANGEETHA P. AND MALLANNARA S. SIDDESHA *

Abstract. This paper investigates almost Ricci-Bourguignon solitons on Lorentzian para-Kenmotsu (LP-Kenmotsu) manifolds. We show that when the soliton vector field coincides with the timelike vector field, the manifold admits an Einstein structure with constant scalar curvature, and the soliton is classified as shrinking or expanding depending on the soliton parameter. In the gradient case, the structure reduces either to an Einstein manifold or a gradient $u^{\#}$-Yamabe soliton. For manifolds of constant scalar curvature, we establish that the geometry is locally isometric to a Lorentzian hyperbolic space, while the Ricci-Bourguignon condition further yields a gradient conformal structure. These results provide a classification of almost Ricci-Bourguignon solitons in the LP-Kenmotsu setting and open avenues for exploring their role in Lorentzian paracontact geometry and spacetime models inspired by general relativity.

Keywords: LP-Kenmotsu manifolds, Ricci-Bourguignon solitons, Einstein manifolds.
2020 Mathematics Subject Classification: 53C25, 53C44, 53C21.

1. Introduction

The concept of geometric flows has become an important tool in modern differential geometry and mathematical physics. Among them, the Ricci flow, introduced by Hamilton [11], plays a central role, as it smooths out irregularities of the metric and leads to self-similar solutions known as Ricci solitons, which generalize Einstein metrics and provide insights into singularity formation in geometry and cosmology. Since then, Ricci solitons have been widely examined in both Riemannian and Lorentzian settings due to their applications in general relativity and cosmology [18].

To capture more general behaviors of evolving metrics, several extensions of Ricci solitons have been introduced. Pigola et al. [23] studied Ricci almost solitons, where the soliton constant is allowed to be a smooth function instead of a fixed constant. Later, Ricci–Yamabe solitons were proposed as a unifying framework involving both Ricci and Yamabe flows [13], and they were also investigated on LP-Kenmotsu manifolds in [12]. In addition, Bourguignon [4]

Received: 2025.09.05 *Revised: 2025.10.07* *Accepted: 2025.10.16*

* Corresponding author
Swapna Sangeetha Prabhakaran ⋄ swapnamath4@gmail.com ⋄ https://orcid.org/0009-0003-5581-2786
Mallannara Siddalingappa Siddesha ⋄ mssiddesha@gmail.com ⋄ https://orcid.org/0000-0003-2367-0544

introduced a modified Ricci flow, known as the Ricci-Bourguignon flow, obtained by adding a scalar curvature term to the Ricci tensor. In this direction, Haseeb and Prasad [14] investigated curvature properties and metric connections specific to LP-Kenmotsu manifolds, providing essential structural insights that underpin soliton behavior. Complementing this, Ahmad et al. [1] studied ρ-Einstein solitons within the framework of LP-Kenmotsu manifolds, focusing on their geometric properties and the conditions under which these solitons exist. Their work contributes to the understanding of Ricci-type solitons in Lorentzian geometry, particularly in the context of para-Kenmotsu structures. Later, Siddesha and Sangeetha [31] extended this work to Riemannian manifolds with concurrent-recurrent vector fields (Riemannian CR manifolds) and further examined the properties of conharmonic and conformal curvature tensors on such manifolds admitting ρ-Einstein solitons. Dwivedi [9] introduced the notion of Ricci-Bourguignon almost solitons and established several results pertaining to it by deriving integral formulas for compact gradient cases and showing that, under suitable curvature or symmetry conditions, such solitons are isometric to Euclidean spheres. Building on this, Dey and Suh [8] studied almost $\star$-$u^{\#}$-Ricci-Bourguignon solitons in the framework of almost contact metric manifolds, particularly Kenmotsu manifolds. They showed that if such a manifold admits an almost $\star$-$u^{\#}$-Ricci-Bourguignon solitons with the potential vector field collinear to the timelike vector field, then the manifold is $u^{\#}$-Einstein. Recently, Naveen Kumar et al. [21] investigated generalized Ricci-type solitons on LP-Kenmotsu manifolds and demonstrated that such a manifold attains Einstein status when its metric conforms to a generalized Ricci-type soliton. For further insights, we suggest [3,5–7,15,16,22–30,32,35]. These generalizations illustrate the richness of soliton theory and motivate the following definition of almost Ricci-Bourguignon solitons:

Definition 1.1. *Let (M, g) be a smooth pseudo-Riemannian manifold. The metric g is said to define an almost Ricci-Bourguignon soliton if there exists a smooth function λ such that the Ricci tensor S of M satisfies*

$$\pounds_V g + 2S + 2(\lambda - \rho r)g = 0, \tag{1.1}$$

where $\pounds_V g$ denotes the Lie derivative of g with respect to a vector field V.

These solitons are classified as shrinking, steady, or expanding according to the sign of λ. If λ is constant, the soliton is referred to as a Ricci-Bourguignon soliton. Furthermore, when V is a Killing vector field, an almost Ricci-Bourguignon soliton reduces to a Ricci-Bourguignon soliton. If the vector field V is the gradient of a smooth function f, i.e., $V = \nabla f$, then the soliton is called a gradient almost Ricci-Bourguignon soliton, and the governing equation becomes

$$\nabla^2 f + S + (\lambda - \rho r)g = 0, \tag{1.2}$$

where S is the Ricci tensor, r is the scalar curvature, ρ a real parameter, and λ a constant.

Having introduced the framework of almost Ricci-Bourguignon solitons, we now place them in the Lorentzian setting, which provides a natural foundation for spacetime models in general relativity. Several recent works have explored soliton structures on Lorentzian manifolds. For instance, the interplay between Cotton and Bach tensors has been studied, leading to characterizations of quasi-Einstein Lorentzian manifolds and their conformal properties [19].

Likewise, the role of semi-symmetric metric connections in defining and classifying Ricci almost solitons has been analyzed [18]. These results illustrate how Lorentzian manifolds extend classical soliton theory to physically relevant settings.

Within this framework, LP-Kenmotsu manifolds appear as a natural generalization of contact-type structures in Lorentzian geometry. Their curvature properties and compatibility with soliton structures have been investigated in several recent works, especially in relation to Ricci–Yamabe solitons [12]. LP-Kenmotsu manifolds are always odd-dimensional and display rich geometric behavior driven by the timelike vector field.

Motivated by these developments, the present work is devoted to the study of almost Ricci-Bourguignon solitons on LP-Kenmotsu manifolds. We examine conditions under which such solitons yield Einstein structures, gradient solitons, or Lorentzian hyperbolic spaces. Our results contribute to the classification of soliton structures in Lorentzian geometry and suggest potential connections with spacetime models in general relativity.

The structure of the paper is as follows: Section 2 provides a review of the basic facts on LP-Kenmotsu manifolds. Section 3 develops the framework of almost Ricci-Bourguignon solitons and presents the main classification results under different geometric conditions. Section 4 is devoted to the gradient case and its consequences. Finally, Section 5 gives the summary of the results obtained and outlines possible directions for future work.

2. LP-Kenmotsu Manifolds

Consider a differentiable manifold M of dimension $(2n+1)$. A Lorentzian almost paracontact metric structure on M is given by a tensor field ϕ of $(1,1)$-type, a vector field u, a 1-form $u^{\#}$, and a Lorentzian metric g, which satisfy the following conditions [2, 20]:

$$\phi^2 = I + u^{\#} \otimes u, \quad u^{\#}(u) = -1, \quad u^{\#} \circ \phi = 0, \tag{2.3}$$

$$g(\phi\zeta_1, \phi\zeta_2) = g(\zeta_1, \zeta_2) + u^{\#}(\zeta_1)u^{\#}(\zeta_2), \quad g(\zeta_1, u) = u^{\#}(\zeta_1), \tag{2.4}$$

$\forall$ vector fields $\zeta_1, \zeta_2 \in \chi(M)$, where I denotes the identity map on the tangent bundle of M. The quadruple $(\phi, u, u^{\#}, g)$ is then called a Lorentzian almost paracontact metric structure.

Such a manifold M is said to be an *LP-Kenmotsu manifold* if its structure tensors satisfy

$$(\nabla_{\zeta_1}\phi)\zeta_2 = -g(\phi\zeta_1, \zeta_2)u - u^{\#}(\zeta_2)\phi\zeta_1, \tag{2.5}$$

for all $\zeta_1, \zeta_2 \in \chi(M)$, here ∇ denotes the Levi-Civita connection associated with g. From relation (2.5), it follows that

$$\nabla_{\zeta_1} u = -\zeta_1 - u^{\#}(\zeta_1)u, \tag{2.6}$$

$$(\nabla_{\zeta_1} u^{\#})\zeta_2 = -g(\zeta_1, \zeta_2) - u^{\#}(\zeta_1)u^{\#}(\zeta_2). \tag{2.7}$$

Furthermore, in any LP-Kenmotsu manifold the following curvature relations hold [14]:

$$u^{\#}(R(\zeta_1, \zeta_2)\zeta_3) = g(\zeta_2, \zeta_3)u^{\#}(\zeta_1) - g(\zeta_1, \zeta_3)u^{\#}(\zeta_2), \tag{2.8}$$

$$R(\zeta_1, \zeta_2)u = u^{\#}(\zeta_2)\zeta_1 - u^{\#}(\zeta_1)\zeta_2, \tag{2.9}$$

$$R(u, \zeta_1)\zeta_2 = g(\zeta_1, \zeta_2)u - u^{\#}(\zeta_2)\zeta_1, \tag{2.10}$$

$$R(u, \zeta_1)u = \zeta_1 + u^{\#}(\zeta_1)u, \tag{2.11}$$

$$S(\zeta_1, u) = 2nu^{\#}(\zeta_1), \tag{2.12}$$

$$Qu = 2nu, \tag{2.13}$$

where R is the Riemannian curvature tensor, S and Q are the Ricci tensor and Ricci operator, respectively.

A $(2n+1)$-dimensional LP-Kenmotsu manifold is called *Einstein* if its Ricci tensor is a scalar multiple of the metric tensor, i.e., $S = fg$ for some smooth function f. According to Li et al. [17], any $(2n+1)$-dimensional LP-Kenmotsu manifold also satisfies the identities

$$(\nabla_{\zeta_1} Q)u = Q\zeta_1 - 2n\zeta_1, \tag{2.14}$$

$$(\nabla_u Q)\zeta_1 = 2Q\zeta_1 - 4n\zeta_1. \tag{2.15}$$

3. Almost Ricci-Bourguignon Solitons on LP-Kenmotsu Manifolds

In this section, we study almost Ricci-Bourguignon solitons on LP-Kenmotsu manifolds. Ahmad et al. [1] recently investigated ρ-Einstein solitons in the Lorentzian para-Kenmotsu setting and showed that such manifolds are necessarily $u^{\#}$-Einstein. For constant scalar curvature, they obtained the soliton constant as

$$\lambda = \rho(n^2 - 1),$$

and the Ricci tensor

$$S(\zeta_1, \zeta_2) = (\lambda - \rho r)g(\zeta_1, \zeta_2) + (\rho r)\, u^{\#}(\zeta_1)u^{\#}(\zeta_2),$$

revealing a quasi-Einstein structure.

Motivated by this, we establish that if the potential vector field V is parallel to the timelike vector field u, then the soliton is trivial and the manifold becomes Einstein with scalar curvature $r = 2n(2n+1)$. We also identify a condition under which the almost Ricci-Bourguignon soliton reduces to a Ricci-Bourguignon soliton, thus aligning with the conclusions of Ahmad et al. [1].

Theorem 3.1. *Let M be a $(2n+1)$-dimensional (>3) LP-Kenmotsu manifold. If its metric g admits an almost Ricci-Bourguignon soliton with potential vector field $V = \sigma u$, where u is the unit timelike vector field and σ is a smooth function, then:*

- *M is an Einstein manifold,*
- *the scalar curvature $r = 2n(2n+1)$,*
- *the gradient $\nabla\sigma$ is collinear with u.*

Proof. Let the metric g on M represent an almost Ricci-Bourguignon soliton. In this case, M satisfies equation (1.1). Since the potential vector field V is parallel to the unit timelike vector field u, it can be expressed as $V = \sigma u$, where σ is a non-zero smooth function defined on M. Therefore, we obtain

$$\nabla_{\zeta_1} V = \zeta_1(\sigma)u + \sigma(-\zeta_1 - u^{\#}(\zeta_1)u),$$

where the covariant derivative of V along $\zeta_1 \in \Gamma(TM)$ has been computed using equation (2.6). Utilizing the foregoing equation in (1.1), we find

$$2S(\zeta_1, \zeta_2) + \zeta_1(\sigma)u^{\#}(\zeta_2) + \zeta_2(\sigma)u^{\#}(\zeta_1) = 2(\sigma - \lambda + \rho r)g(\zeta_1, \zeta_2) + 2\sigma u^{\#}(\zeta_1)u^{\#}(\zeta_2), \tag{3.16}$$

$\forall\ \zeta_1, \zeta_2 \in \chi(M)$. Now, substituting u in place of ζ_2 in the preceding equation and applying relation (2.12), we obtain

$$\zeta_1(\sigma) = [u(\sigma) + 2(2n + \lambda - \rho r)]u^{\#}(\zeta_1),\ \ \zeta_1 \in \chi(M). \tag{3.17}$$

Assigning $\zeta_1 = u$ in equation (3.17) yields $\lambda - \rho r = -[u(\sigma) + 2n]$. Plugging this result back into equation (3.17), we get

$$\zeta_1(\sigma) = -u(\sigma)u^{\#}(\zeta_1),\ \ \zeta_1 \in \chi(M), \tag{3.18}$$

where

$$u(\sigma) = -\lambda + \rho r - 2n. \tag{3.19}$$

As a result of equation (3.18) and the relation $\lambda - \rho r = -[u(\sigma) + 2n]$, equation (3.16) takes the form

$$S(\zeta_1, \zeta_2) = [\sigma + u(\sigma) + 2n]g(\zeta_1, \zeta_2) + [u(\sigma) + \sigma]u^{\#}(\zeta_1)u^{\#}(\zeta_2),\ \ \zeta_1, \zeta_2 \in \chi(M). \tag{3.20}$$

Let $\{e_i\}_{i=1}^n$ be a local orthonormal basis on M. By substituting $\zeta_1 = \zeta_2 = e_i$ into the above equation and taking sum over i, we obtain

$$\sigma + u(\sigma) = \frac{r}{2n} - (2n + 1). \tag{3.21}$$

Substituting equation (3.21) into equation (3.20) yields

$$S(\zeta_1, \zeta_2) = \Big(\frac{r}{2n} - 1\Big)\, g(\zeta_1, \zeta_2) + \Big(\frac{r}{2n} - (2n + 1)\Big)\, u^{\#}(\zeta_1)u^{\#}(\zeta_2). \tag{3.22}$$

Therefore, M is a quasi-Einstein manifold. Using the quasi-Einstein condition, it has been demonstrated that the scalar curvature r of M with dimension greater than 3 satisfies the following equation (see Lemma (2.5) of [13]):

$$\zeta_1(r) = -u(r)u^{\#}(\zeta_1),\ \ \zeta_1 \in \chi(M). \tag{3.23}$$

Furthermore, by differentiating equation (3.22) covariantly with respect to ζ_3 and applying relation (2.6), we obtain

$$\begin{aligned}(\nabla_{\zeta_3} S)(\zeta_1, \zeta_2) \ &= \ -\Big(\frac{r}{2n} - (2n + 1)\Big)\, [g(\zeta_1, \zeta_3)u^{\#}(\zeta_2) + g(\zeta_2, \zeta_3)u^{\#}(\zeta_1) \\ &\quad +2u^{\#}(\zeta_1)u^{\#}(\zeta_2)u^{\#}(\zeta_3)] + \frac{\zeta_3(r)}{2n}[g(\zeta_1, \zeta_2) \\ &\quad +u^{\#}(\zeta_1)u^{\#}(\zeta_2)],\ \ \zeta_1, \zeta_2 \in \chi(M).\end{aligned} \tag{3.24}$$

By contracting equation (3.24) over ζ_2 and ζ_3, and then applying equation (3.23), we get

$$u(r) = 2[r - (2n + 1)(2n)]. \tag{3.25}$$

Assuming that the unit timelike vector field u leaves the scalar curvature r invariant which means $ur = 0$, from relation (3.25) it follows that $r = (2n + 1)(2n)$, which indicates that the scalar curvature is constant. Consequently, from equation (3.22), we deduce

$$S(\zeta_1, \zeta_2) = (2n)g(\zeta_1, \zeta_2),\ \zeta_1, \zeta_2 \in \chi(M).$$

Thus, M is an Einstein manifold. Given $r = (2n+1)(2n)$, equation (3.21) implies $u(\sigma) = -\sigma$, thereby concluding the proof of the theorem. □

Now, if σ is assumed to be a non-zero constant rather than a function, equation (3.19) simplifies to $\lambda = \rho r - 2n$, which is a constant. Substituting the value of r into this expression gives

$$\lambda = 2n[\rho(2n+1) - 1].$$

This shows that λ is positive if $\rho > 0$ and negative if $\rho < 0$. Accordingly, we present the following corollary:

Corollary 3.1. *If the metric g of a $(2n+1)$-dimensional $((2n+1) > 3)$ LP-Kenmotsu manifold M represents an almost Ricci-Bourguignon soliton where the non-zero potential vector field V is a constant multiple of the unit timelike vector field u, then the soliton is classified as shrinking if $\rho > 0$ or expanding if $\rho < 0$.*

4. Gradient Almost Ricci-Bourguignon Solitons on LP-Kenmotsu Manifolds

In this section, we analyze the nature of gradient almost Ricci-Bourguignon solitons on LP-Kenmotsu manifolds. Prior studies, such as [34], have shown that in three-dimensional Kenmotsu geometry, the existence of gradient almost Ricci solitons leads either to constant negative curvature or forces the potential field to align with the timelike vector field. Similar conclusions were drawn in [10], where the soliton was found to be expanding and the manifold was shown to be $u^{\#}$-Einstein. Since LP-Kenmotsu manifolds provide a Lorentzian analogue to Kenmotsu structures, extending these results to the LP-setting offers deeper geometric insights. We establish the following theorem.

Theorem 4.1. *Let M be an LP-Kenmotsu manifold whose metric g admits a gradient almost Ricci-Bourguignon soliton. Then M is either Einstein or the metric defines a gradient $u^{\#}$-Yamabe soliton.*

Proof. Assume that the Lorentzian metric g on the manifold M admits a gradient almost Ricci-Bourguignon soliton structure. Then, by applying equation (1.2), we obtain

$$\nabla_{\zeta_1}\nabla f + Q\zeta_1 = (-\lambda + \rho r)\zeta_1, \quad \zeta_1 \in \chi(M), \tag{4.26}$$

where f is the potential function. Taking the curvature operator into account and differentiating appropriately yields

$$R(\zeta_1, \zeta_2)\nabla f = (\nabla_{\zeta_2}Q)\zeta_1 - (\nabla_{\zeta_1}Q)\zeta_2 + \zeta_1(-\lambda + \rho r)\zeta_2 - \zeta_2(-\lambda + \rho r)\zeta_1. \tag{4.27}$$

Replacing the vector field ζ_1 with the unit timelike vector field u in the above expression and utilizing identity (2.10), we arrive at

$$(\zeta_2 f)u - (uf)\zeta_2 = (\nabla_{\zeta_2}Q)u - (\nabla_u Q)\zeta_2 + u(-\lambda + \rho r)\zeta_2 - \zeta_2(-\lambda + \rho r)u. \tag{4.28}$$

Furthermore, utilizing equations (2.14) and (2.15), we obtain the following identities involving the Ricci operator Q

$$g(\zeta_2, \nabla(f - \lambda + \rho r))u - u(f - \lambda + \rho r)\zeta_2 = 2n\zeta_2 - Q\zeta_2. \tag{4.29}$$

By contracting with u and simplifying, one finds:

$$d(f - \lambda + \rho r) = -u(f - \lambda + \rho r)u^{\#}, \tag{4.30}$$

where d is the exterior derivative. This shows that the function $f-\lambda+\rho r$ remains constant along the distribution $\mathcal{D}$ orthogonal to the unit timelike vector field u. Substituting equation (4.30) into (4.29), we deduce that

$$-u(f-\lambda+\rho r)\{u^{\#}(\zeta_2)u+\zeta_2\}=2n\zeta_2-Q\zeta_2. \tag{4.31}$$

Now, taking the trace of the above equation yields

$$u(f-\lambda+\rho r)=\left((2n+1)-\frac{r}{2n}\right). \tag{4.32}$$

Inserting (4.32) into (4.31), one immediately obtains an $u^{\#}$-Einstein condition (3.22). Further computations provide:

$$S(\zeta_2,\nabla f)=\left(\frac{r}{2n}-1\right)\zeta_2 f+\left(\frac{r}{2n}-(2n+1)\right)(uf)u^{\#}(\zeta_2). \tag{4.33}$$

Subsequently, by tracing equation (4.27) along ζ_1 yields

$$S(\zeta_2,\nabla f)=\frac{1}{2}\zeta_2(r)-2n\zeta_2(-\lambda+\rho r).$$

Equating the preceding expressions, we observe that

$$\zeta_2(r)=4n\zeta_2(-\lambda+\rho r)+2\left(\frac{r}{2n}-1\right)(\zeta_2 f)+2\left(\frac{r}{2n}-(2n+1)\right)(uf)u^{\#}(\zeta_2). \tag{4.34}$$

From this, one infers that $dr\wedge u^{\#}=0$, and hence

$$\zeta_2(r)=2[2n(2n+1)-r]u^{\#}(\zeta_2). \tag{4.35}$$

Now, assume that the vector field ζ_2 in equation (4.34) belongs to the distribution $\mathcal{D}$, orthogonal to u. Since $f-\lambda+\rho r$ is constant along $\mathcal{D}$, and using identities (4.30) and (4.35), we arrive at $\{2n(2n+1)-r\}(\zeta_2 f)=0$, for every $\zeta_2\in\mathcal{D}$. As a result, it follows that

$$(2n(2n+1)-r)(\nabla f+(uf)u)=0. \tag{4.36}$$

If $r=2n(2n+1)$, then by equation (3.22), the Ricci tensor reduces to $S(\zeta_1,\zeta_2)=2n\,g(\zeta_1,\zeta_2)$, and thus the manifold M is Einstein. On the other hand, if $r\neq 2n(2n+1)$ on some open subset $\mathcal{O}\subset M$, then equation (4.36) implies that $\nabla f=-(uf)u$. This alignment of the gradient with the unit timelike vector field leads to the relation $df=-(uf)u^{\#}$. Taking the exterior derivative of this expression yields $d^2f=-[d(uf)\wedge u^{\#}+(uf)du^{\#}]=0$, from which it follows that uf is constant, as $d^2f=0$ and $du^{\#}=0$ on an LP-Kenmotsu manifold. Differentiating the relation $\nabla f=-(uf)u$ covariantly along a vector field ζ_2 yields $\nabla_{\zeta_2}\nabla f=-\zeta_2(uf)u-(uf)(-\zeta_2-u^{\#}(\zeta_2)u)$, so that $\mathrm{Hess}(f)=(uf)(g+u^{\#}\otimes u^{\#})$. This confirms that the structure corresponds to a gradient $u^{\#}$-Yamabe soliton, which completes the proof. □

Moreover, when the scalar curvature satisfies $r=2n(2n+1)$, the manifold M becomes Einstein, and this scalar curvature remains constant. Substituting this value into equation (4.32), we find that $u(f)=u(\lambda-\rho r)$, which implies that $\nabla f=\nabla(\lambda-\rho r)$. As a result, the equation (4.26) reduces to

$$\nabla_{\zeta_2}\nabla(\lambda-\rho r)=(-\lambda+\rho r-2n)\zeta_2,\quad \text{for all } \zeta_2\in\chi(M).$$

Applying Theorem 2 of Tashiro [33], we conclude that if the manifold M is complete, then it is locally isometric to the hyperbolic space $\mathbb{H}^{2n+1}$.

Corollary 4.1. *Let M be a complete $(2n+1)$-dimensional LP-Kenmotsu manifold with constant scalar curvature admitting a gradient almost Ricci-Bourguignon soliton. Then M is locally isometric to a Lorentzian hyperbolic space, provided $\nabla f \neq -(uf)u$.*

If the soliton is a Ricci-Bourguignon soliton (i.e., λ is constant), then the soliton equation becomes:

$$\nabla^2 f = \mu g, \quad \text{with} \quad \mu = -\lambda + \rho r - 2n,$$

implying the soliton is gradient conformal.

Corollary 4.2. *If an LP-Kenmotsu manifold with constant scalar curvature admits a gradient Ricci-Bourguignon soliton, then the manifold is gradient conformal.*

5. Conclusion

In this work, we investigated almost Ricci-Bourguignon solitons on LP-Kenmotsu manifolds. We showed that when the soliton vector field is aligned with the timelike vector field, the manifold becomes Einstein with constant scalar curvature, and the soliton is classified as shrinking or expanding depending on the parameter. In the gradient case, the geometry reduces either to an Einstein structure or to a gradient $u^{\#}$-Yamabe soliton. For constant scalar curvature, the manifold is locally isometric to a Lorentzian hyperbolic space, while in the case of a Ricci-Bourguignon soliton, the metric additionally admits a gradient conformal structure. Overall, these results provide a classification of Ricci-Bourguignon solitons in the LP-Kenmotsu setting and motivate further extensions to other paracontact geometries. Future work may also explore their physical interpretations in spacetime models inspired by general relativity.

Acknowledgments. The authors would like to thank the referee for some useful comments and their helpful suggestions that have improved the quality of this paper.

References

[1] Ahmad, M., Bilal, M., & Gazala. (2024). ρ-Einstein solitons in Lorentzian para-Kenmotsu manifolds. *Results in Nonlinear Analysis*, 7(2), 53–63.

[2] Alegre, P. (2013). Slant submanifolds of Lorentzian Sasakian and Para-Sasakian manifolds. *Taiwanese Journal of Mathematics*, 17(3), 897–910.

[3] Bagewadi, C. S., Nirmala, D., & Siddesha, M. S. (2018). Semi-invariant submanifolds of $(LCS)_n$-manifold. *Communications of the Korean Mathematical Society*, 33(4), 1331–1339.

[4] Bourguignon, J. P. (1981). Ricci curvature and Einstein metrics. In *Global Differential Geometry and Global Analysis* (Lecture Notes in Mathematics), Springer, 838, 42–63.

[5] Chaudhary, R. S., & Pal, B. (2025). Gradient Ricci–Bourguignon solitons and applications. *Afrika Matematika*, 36(1), 25.

[6] De, K., Khan, M. N. I., De, U. C., & Li, Y. (2025). Ricci–Bourguignon solitons with certain applications to relativity. *Journal of Mathematics*, 2025(1), 4866447.

[7] De, U. C., & De, K. (2024). K-Ricci–Bourguignon almost solitons. *International Electronic Journal of Geometry*, 17(1), 63–71.

[8] Dey, S., & Suh, Y. J. (2023). Geometry of almost contact metrics as an almost $*$-η-Ricci–Bourguignon soliton. *Reviews in Mathematical Physics*, 35(7), 2350012.

[9] Dwivedi, S. (2021). Some results on Ricci–Bourguignon solitons and almost solitons. *Canadian Mathematical Bulletin*, 64(3), 591–604.

[10] Ghosh, A. (2019). Ricci soliton and Ricci almost soliton within the framework of Kenmotsu manifold. *Carpathian Mathematical Publications*, 11(1), 59–69.

[11] Hamilton, R. S. (1982). Three-manifolds with positive Ricci curvature. *Journal of Differential Geometry*, 17(2), 255–306.

[12] Haseeb, A., Bilal, M., Chaubey, S. K., & Ahmadini, A. A. H. (2022). ζ-Conformally Flat LP-Kenmotsu Manifolds and Ricci–Yamabe Solitons. *Mathematics*, 11(1), 212.

[13] Haseeb, A., Mofarreh, F., Chaubey, S. K., & Prasad, R. (2024). A study of $*$-Ricci–Yamabe solitons on LP-Kenmotsu manifolds. *AIMS Mathematics*, 9(8), 22532-22546.

[14] Haseeb, A., & Prasad, R. (2021). Certain results on Lorentzian para-Kenmotsu manifolds. *Boletim da Sociedade Paranaense de Matemática*, 39(3), 201–220.

[15] Khatri, M., & Singh, J. P. (2024). Ricci–Bourguignon soliton on three-dimensional contact metric manifolds. *Mediterranean Journal of Mathematics*, 21(2), 70.

[16] Kishor, S., Bhardwaj, A. K., Mani, N., & Shukla, R. (2025). Lorentzian para-Kenmotsu manifolds within the framework of $*-$conformal η-Ricci soliton. *Journal of Applied Mathematics*, 2025(1), 6684661.

[17] Li, Y., Haseeb, A., & Ali, M. (2022). LP-Kenmotsu Manifolds Admitting η-Ricci Solitons and Spacetime. *Journal of Mathematics*, 2022(1), 6605127.

[18] Li, Y., Kumara, H. V., Siddesha, M. S., & Naik, D. M. (2023). Characterization of Ricci almost soliton on Lorentzian manifolds. *Symmetry*, 15(6), 1175.

[19] Li, Y., Siddesha, M. S., Kumara, H. V., & Praveena, M. M. (2024). Characterization of Bach and Cotton tensors on a class of Lorentzian manifolds. *Mathematics*, 12(19), 3130.

[20] Matsumoto, K. (1989). On Lorentzian paracontact manifolds. *Bulletin of the Yamagata University, Natural Science*, 12, 151–156.

[21] Naveen Kumar, R. T., Siddesha, M. S., Swapna Sangeetha, P., Sowmyashree, B. M., & Siva Kota Reddy, P. (2025). Characterization of generalized Ricci-type solitons on Lorentzian para-Kenmotsu manifolds. *Dynamics of Continuous, Discrete and Impulsive Systems, Series A: Mathematical Analysis*, 32, 271–281.

[22] Pankaj, P., Chaubey, S. K., & Prasad, R. (2021). Three-dimensional Lorentzian para-Kenmotsu manifolds and Yamabe solitons. *Honam Mathematical Journal*, 43(4), 613–626.

[23] Pigola, S., Rigoli, M., Rimoldi, M., & Setti, A. G. (2011). Ricci almost solitons. *Annali della Scuola Normale Superiore di Pisa-Classe di Scienze*, 10(4), 757–799.

[24] Prakasha, D. G., Amruthalakshmi, M. R., & Suh, Y. J. (2024). Geometric characterizations of almost Ricci–Bourguignon solitons on Kenmotsu manifolds. *Filomat*, 38(3), 861–871.

[25] Prasad, R., Haseeb, A., Verma, A., & Yadav, V. S. (2024). A study of φ- Ricci symmetric LP-Kenmotsu manifolds. *International Journal of Maps in Mathematics*, 7(1), 33–44.

[26] Prasad, R., Verma, A., Yadav, V. S., Haseeb, A., & Bilal, M. (2024). LP-Kenmotsu Manifolds Admitting Bach Almost Solitons. *Universal Journal of Mathematics and Applications*, 7(3), 102–110.

[27] Praveena, M. M., & Siddesha, M. S. (2025). Conformal solitons in relativistic magneto-fluid spacetimes with anti-torqued vector fields. *International Journal of Maps in Mathematics*, 8(2), 642–652.

[28] Praveena, M. M., Siddesha, M. S., & Bagewadi, C. S. (2022). Certain results of Ricci solitons on (LCS) manifolds. *International Journal of Maps in Mathematics*, 5(2), 101–111.

[29] Shenawy, S., Bin Turki, N., Syied, N., & Mantica, C. (2023). Almost Ricci–Bourguignon solitons on doubly warped product manifolds. *Universe*, 9(9), 396.

[30] Siddesha, M. S., Bagewadi, C. S., Nirmala, D., & Srikantha, N. (2017). On the geometry of pseudoslant submanifolds of LP-cosymplectic manifold. *International Journal of Mathematics And its Applications*, 5(4), 81–87.

[31] Siddesha, M. S., & Sangeetha, P. S. (2025). Riemannian CR manifolds and ρ-Einstein solitons: A geometric analysis and applications. *International Journal of Maps in Mathematics*, 8(1), 309–325.

[32] Soylu, Y. (2022). Ricci–Bourguignon solitons and almost solitons with concurrent vector field. *Differential Geometry–Dynamical Systems*, 24, 191–200.

[33] Tashiro, Y. (1965). Complete Riemannian manifolds and some vector fields. *Transactions of the American Mathematical Society*, 117, 251–275.

[34] Wang, Y. (2016). Gradient Ricci almost solitons on two classes of almost Kenmotsu manifolds. *Journal of the Korean Mathematical Society*, 53(5), 1101–1114.

[35] Yano, K. (1970). Integral formulas in Riemannian geometry. (Vol. 1) *Marcel Dekker*, New York.

(P. Swapna Sangeetha, M. S. Siddesha) Department of Data Analytics and Mathematical Science, Faculty of Engineering and Technology, Jain (Deemed-to-be University), Global Campus-562112, Karnataka, INDIA.

CALCULATION

Volume ***2****, Issue* ***1****, 2026, Pages:****12–25***

E-ISSN: 3062–2107

www.simadp.com/calculation

$\widetilde{L_r}-$FINITE TYPE NULL HYPERSURFACES IN GENERALIZED ROBERTSON-WALKER SPACETIMES

EZECHIEL ADEDEMI, CYRIAQUE ATINDOGBÉ *, AND RAYMOND HOUNNONKPÈ

Abstract. This paper explores the $\widetilde{L_r}$-finite type null hypersurfaces within generalized Robertson-Walker spacetimes, where $\widetilde{L_r}$ stands for the linearized operator of the first variation of the $(r+1)-$th mean curvature arising from normal variations of the hypersurface equipped with its rigged Riemannian structure. We provide necessary and/or sufficient conditions characterizing $\widetilde{L_r}$-p-type and $\widetilde{L_r}$-null-p-type null hypersurfaces ($p = 1, 2$), followed by various examples.

Keywords: $\widetilde{L_r}-$finite type null hypersurfaces, isoparametric, Generalized Robertson-Walker spacetime

2020 Mathematics Subject Classification: 53C40, 53C42.

1. Introduction

In the late 1970s, while interested in finding the best possible estimate of the total mean curvature of a compact submanifold in Euclidean space and to define a notion of degree for these submanifolds, Chen, B. Y. introduced the concept of finite type submanifolds ([6]). Since then, this field in differential geometry associated with position vector fields has evolved very fastly as highlighted in the comprehensive survey by Chen, B.-Y [7, Chapter 6].

A submanifold $\psi : M^n \to \mathbb{R}^{n+k}$ is said to be of finite type if the position vector field ψ has the following spectral decomposition

$$\psi = \psi_0 + \psi_1 + \cdots + \psi_p \quad \text{with } \Delta\psi_i = \lambda_i\psi_i, \tag{1.1}$$

for some positive integer $p \in \mathbb{N}$, such that $\psi_0 \in \mathbb{R}^{n+k}$ is a constant vector, ψ_i $(i = 1, \dots p)$ are non-constant $\mathbb{R}^{n+k}-$valued maps on M^n and $\lambda_i \in \mathbb{R}$ for each i, where Δ is the Laplacian operator on M. If all $\lambda_i's$ $(i = 1, \cdots p)$ are mutually distinct, the submanifold M^n is termed p-type, and if any of them is zero, M is called null$-p-$type.

Received: 2025.10.05 *Accepted: 2025.12.19*

* Corresponding author

Ezechiel Adedemi ⋄ rodrigueadedemi@gmail.com ⋄ https://orcid.org/0009-0002-0208-4861

Cyriaque Atindogbé ⋄ atincyr@gmail.com ⋄ https://orcid.org/0000-0001-8346-4027

Raymond Hounnonkpe ⋄ rhounnonkpe@ymail.com ⋄ https://orcid.org/0000-0002-5013-8329

It is well-known that the Laplacian operator for an isometrically immersed hypersurface $M^n \subset \mathbb{R}^{n+1}$ is an intrinsic second-order linear differential operator. It naturally arises as the linearized operator of the first variation of the mean curvature for normal variations of the hypersurface. Thus, the Laplacian operator Δ can be considered as the first in a series of n operators $L_0 = \Delta, L_1, \ldots, L_{n-1}$, where L_r represents the linearized operator of the first variation of the $(r+1)$-th order mean curvature due to normal variations. These operators are defined by

$$L_r(f) = \mathrm{tr}(T_r \circ \nabla^2 f),$$

for any smooth function f on M, where T_r denotes the r-th Newton transformation associated with the shape operator of the hypersurface, and $\nabla^2 f$ is metrically dual operator to the Hessian of f. Although generally not elliptic, the operators L_r share properties with the Laplacian operator of M, as discussed in [1] and the concepts of finite $p-$type and null$-p-$type extend naturally in $L_k - p-$type and $L_k -$ null $- p-$type, respectively for pseudo-Riemannian submanifolds M_t^n in the pseudo-Euclidean spaces $\mathbb{R}_s^m$. In [11], the authors study L_k-finite type hypersurfaces in the hyperbolic space $\mathbb{H}^{n+1} \subset \mathbb{R}_1^{n+2}$ for $k \geqslant 1$, examining properties specific to these spaces, such as the principal curvatures and operators associated with hyperbolic geometry. They also address results related to specific cases of hypersurfaces in larger hyperbolic spaces, exploring geometric consequences, particularly for totally umbilical and k-minimal hypersurfaces. A key result stands as follows : k-minimal H_k-hypersurfaces in $\mathbb{H}^4$ and open portions of a non-flat totally umbilical hypersurface in $\mathbb{H}^4$ are the only $L_k - 1-$ type hypersurfaces in $\mathbb{H}^4$. They also show that if $\psi : M^3 \to \mathbb{H}^4 \subset \mathbb{R}_1^5$ is an orientable H_k-hypersurface, then, if M is of $L_k - 2-$ type, then H_{k+1} is a nonzero constant. In n-dimensional case, they show that orientable H_k-hypersurface M^n that has at most two distinct principal curvatures is of $L_k - 2-$ type if and only if M^n is an open portion of

$$M_m^n(r) = \left\{ (x_1, \ldots, x_{n+2}) \mid -x_1^2 + \sum_{i=2}^{m+1} x_i^2 = -1 - r^2, \sum_{j=m+2}^{n+2} x_j^2 = r^2 \right\},$$

for some positive integer m, $1 \leqslant m \leqslant n-1$, and for some positive number r. It is worth mentioning that, as far as we know, all the hypersurfaces involved in known results are nondegenerate. To contribute filling the gap, the pressent paper aims to explore the null case in Generalized Robertson Walker spacetimes.

In upcoming Section 2, we fix basic normalization equations, isoparametric properties and background informations on Newton transformations and $\widetilde{L}_r-$operators as presented in [2] and [12]. Our main results are located in Section 3 and Section 4. In Section 3, we show that $\widetilde{L_r}$-1-type condition is equivalent to $r-$maximility for null hypersurfaces in de Sitter and anti de Sitter spaces (Theorem 3.1) and similar necessary and sufficient condition for the flat case $c = 0$ (Theorem 3.2). In Section 4, we focused on $\widetilde{L_r} - 2$-type condition. Theorem 4.1 asserts that for non zero constant $\overset{\star}{S}_2$, $c = \pm 1$ and $r = 0, 1, 2$, such null hypersurfaces are necessarily isoparametric. For more general case, Theorem 4.2 asserts that for non-zero constant $\overset{\star}{S}_2$ and $\overset{\star}{S}_r$, $\widetilde{L_r} - Null - 2$-type condition is equivalent to isoparametric when $c = \pm 1$. Finally, we show that in the flat Minkowski space ($c = 0$), the $\widetilde{L_r} - 2$-type condition reduces also to isoparametric one (Theorem 4.3). Different results are supported by various examples.

2. Null Hypersurfaces in GRW Spacetimes

2.1. **Normalization and rigged structure.** A hypersurface M of a Lorentzian manifold $(\overline{M}, \overline{g})$ is null if the metric tensor is degenerate on it, i.e the induced structure from the Lorentzian ambient manifold is degenerate.

A rigging for a null hypersurface M is a vector field ζ defined in some open neighbourhood of M such that $\zeta_p \notin T_pM$ for all $p \in M$. If ζ is defined only over M, then we call it a restricted rigging. If a rigging exists, then we can take the unique null vector field $\xi \in \mathfrak{X}(M)$ such that $\overline{g}(\zeta, \xi) = 1$ (called rigged vector field) and the (screen) distribution given by $\mathcal{S}_p = \zeta_p^{\perp} \cap T_pM$ for all $p \in M$. A rigging with integrable screen distribution $\mathcal{S}$ induces a screen foliation $\mathscr{F}$ and will be termed $\mathscr{F}-$rigging. We can also define the rigged metric as the Riemannian metric on M given by $\widetilde{g} = g + \omega \otimes \omega$, where $\omega = i^*\alpha$, $g = i^\star \overline{g}$ and α the $\overline{g}$-metrically equivalent one-form to ζ with $i : M \to \overline{M}$ the canonical inclusion map. The rigged vector field ξ is unitary and orthogonal to $\mathcal{S}$ with respect to $\widetilde{g}$. Moreover, ω is $\widetilde{g}$-metrically equivalent to ξ, and is called the rigged one-form. The vector field $N = \zeta - \frac{1}{2}\overline{g}(\zeta, \zeta)\xi$ is the unique null vector field defined on M, orthogonal to the screen distribution $\mathcal{S}$ and such that $\overline{g}(N, \xi) = 1$.

Moreover, we have the following decompositions :

$$T_p\overline{M} = T_pM \oplus span(N_p), \quad T_pM = span\{\xi_p\} \oplus \mathcal{S}_p \tag{2.2}$$

for all $p \in M$.

The rigging technique presents two main advantages. The first one is that all the geometric objects defined above from the rigging are tuned together in a way that allows linking properties of the null hypersurface with properties of the ambient space. The second one is the presence of the Riemannian rigged metric $\widetilde{g}$, which geometry is reasonably well coupled with the ambient geometry in most cases and it allows us to use Riemannian tools for the study of the null hypersurface [10].

We get from decompositions (2.2)

$$\overline{\nabla}_U V = \nabla_U V + B(U, V)N, \qquad \overline{\nabla}_U N = -A(U) + \tau(U)N \tag{2.3}$$

where $\overline{\nabla}$, ∇ are the Levi-Civita connection of $\overline{M}$ and the induced (projected) connection on M, respectively. The induced connection ∇ is torsion free but, in general, is not metric, which makes it less useful in the theory. The second fundamental form B, the one-form τ (also called rotation one form) and the screen second fundamental form C are given by

$$B(U, V) = -g(\nabla_U \xi, V), \qquad \tau(U) = -g(\nabla_U \xi, \zeta),$$
$$C(U, V) = -g(\overline{\nabla}_U N, P(V)) = -g(\overline{\nabla}_U \zeta, P(V)),$$

for all $U, V \in \mathfrak{X}(M)$, where $P : TM \to \mathcal{S}$ is the canonical projection associated to the second decomposition in (2.2). The vector field $\overline{\nabla}_U \xi = \nabla_U \xi$ is tangent to the null hypersurface M and can be decomposed as

$$\overline{\nabla}_U \xi = -\tau(U)\xi - \overset{\star}{A}(U),$$

where $\overset{\star}{A}(U) \in \mathcal{S}$. The endomorphism $\overset{\star}{A}$ is the shape operator of $\mathcal{S}$ and satisfies

$$B(U, V) = g(\overset{\star}{A}(U), V) = g(U, \overset{\star}{A}(V)), \qquad B(\xi, U) = 0.$$

Some useful identities in the theory are the following:

$$-2C(U,X) = d\omega(U,X) + (L_\zeta g)(U,X) + g(\zeta,\zeta)B(U,X), \tag{2.4}$$

the Gauss-Codazzi equation

$$\begin{aligned} g(R_{UV}W,\xi) = g(\left(\nabla_U \overset{\star}{A}\right)(V),W) - g(\left(\nabla_V \overset{\star}{A}\right)(U),W) \\ + \tau(U)g(\overset{\star}{A}(V),W) - \tau(V)g(\overset{\star}{A}(U),W), \end{aligned} \tag{2.5}$$

$$(L_\xi \widetilde{g})(X,Y) = -2B(X,Y) \tag{2.6}$$

for all $U,V,W \in \mathfrak{X}(M)$,$X,Y \in \mathcal{S}$, and the Raychaudhuri equation [3, Remark 3] :

$$\overline{Ric}(\xi,\xi) = \xi(H) + \tau(\xi)H - \| \overset{\star}{A} \|^2,$$

where H denotes the (non-normalized) null mean curvature of the null hypersurface given by

$$H_p = \sum_{i=1}^{n} B(e_i,e_i),$$

with $\{e_1,\ldots,e_n\}$ an orthonormal basis in $\mathcal{S}_p$. In particular, $H = -\widetilde{\text{div}}\xi$.

If $B = 0$, then it is said that M is totally geodesic and if $B = \rho g$ for certain $\rho \in C^\infty(M)$, then M is totally umbilical. Observe that these definitions do not depend on the chosen rigging, although the tensors B, τ and C do depend. Throughout, the Levi-Civita connection on the normalized rigged structure $(M,\widetilde{g})$ will be denoted $\widetilde{\nabla}$ and we have for all $X,Y,Z \in \mathcal{S}$

$$C(\xi,X) = -\tau(X) - \widetilde{g}(\widetilde{\nabla}_\xi \xi, X), \qquad \widetilde{\nabla}_X Y = \overset{\star}{\nabla}_X Y - \widetilde{g}(\widetilde{\nabla}_X \xi, Y)\xi,$$

being $\overset{\star}{\nabla}$ the connection on the screen bundle $\mathcal{S}$. In particular

$$\widetilde{g}(\widetilde{\nabla}_X Y, Z) = g(\nabla_X Y, Z) = \overline{g}(\overline{\nabla}_X Y, Z) \quad \forall X,Y,Z \in \mathcal{S}.$$

From now on, we assume $\overline{M}$ to be a generalized Robertson-Walker (GRW) spacetime of constant sectional curvature $c \in \{-1,0,1\}$, which will be denoted $\overline{M}_1^{n+2}(c)$ throughout. We have

$$\overline{M}_1^{n+2}(c) = (I \times_f F, \overline{g}), \quad \overline{g} = -dt^2 + f^2(t)g_F$$

where f (the warping function) is a smooth positive function on I. It is known that such spacetime admits timelike closed and conformal vector field, say $\zeta = f\partial_t$. So, the target space $\overline{M}_1^{n+2}(c)$ of immersion is locally isometric to one of the modele spaces : de Sitter spacetime $\mathbb{S}_1^{n+2}$ of curvature $c = 1$, the Lorentz-Minkowski spacetime $\mathbb{R}_1^{n+2}$ when $c = 0$ or the anti de Sitter spacetime $\mathbb{H}_1^{n+2}$ (actually the universal covering of this pseudohyperbolic space $\mathbb{H}_1^{n+2}$) of curvature $c = -1$. Hence, we consider the following orientable isometric immersion

$$\psi : M^{n+1} \longrightarrow \overline{M}_1^{n+2}(c) \subseteq \mathbb{R}_{1+t}^m$$

of the null hypersurface in $\overline{M}_1^{n+2}(c)$ where $m = n+2+c^2$ and $t = c(c-1)/2$ with $c = 1,0,-1$.

Due to the causal character (spacelike or null) of tangent vectors to a null hypersurface in Lorentzian space, the induced singular metric on the null hypersurface has signature $(0,n)$. So the timelike concircular vector field ζ can act as rigging vector field for M. The closed and conformal vector field ζ has the outstanding property that there exists a smooth function $\sigma \in C^\infty(\overline{M})$ (the conformal factor) such that $\overline{\nabla}_U \zeta = \sigma U$ for all $U \in \mathfrak{X}(\overline{M})$. In particular

$L_\zeta \overline{g} = 2\sigma\overline{g}$. For a closed and conformal rigging, the rotation 1−form vanishes identically ($\tau = 0$) and ξ is $\overline{g}$−geodesic. Moreover, due to the closedness of ζ, $\widetilde{\nabla}_U\xi = -\overset{\star}{A}(U)$ and

$$\widetilde{\nabla}_U V = \nabla_U V + [B(U,V) - C(U,PV)]\,\xi, \tag{2.7}$$

for all $U, V \in \mathfrak{X}(M)$. Also, using (2.4) we derive the following useful relation linking the shape operators A and $\overset{\star}{A}$.

$$A = -\frac{1}{2}\lambda\,\overset{\star}{A} - \sigma P, \tag{2.8}$$

where $\lambda = \overline{g}(\zeta,\zeta)$ denotes the length function of ζ.

For the closed rigging ζ, the screen distribution $p \mapsto \mathcal{S}_p = \zeta_p^\perp \cap T_pM$ is integrable and gives rise to a foliation $\mathscr{F}$ on the null hypersurface. Moreover, we have shown in [4, Lemma 7] that the conformal factor σ and the length function λ are constant through the (screen) leaves $\mathscr{F}_p$, $p \in M$. In other words,

$$X \cdot \sigma = 0 \quad \text{and} \quad X \cdot \lambda = 0$$

for all $X \in \mathcal{S}$.

In [12, 13], null screen isoparametric hypersurfaces are defined to be normalized null hypersurfaces with screen foliation on which the screen principal curvatures are leafwise constant. It is not difficult to see that, if for a given rigging ζ on M, the screen principal curvatures (say) $\overset{\star}{\kappa}_i$ are constant, then for any rigging ζ' for M with associated screen principal curvatures $\overset{\star}{\kappa}_i{}'$, there exists a smooth non vanishing function ϕ on M such that $\phi\overset{\star}{\kappa}_i{}'$ are also constant. This motivates the following definition of isoparametric null hypersurfaces, without prior reference to a fixed normalization.

Definition 2.1. *A null hypersurface M is said to be isoparametric if it admits a $\mathscr{F}$−rigging ζ with associated screen principal curvatures κ_i and a smooth non vanishing function $\phi \in \mathcal{C}^\infty(M)$ such that $\phi\kappa_i$ is leafwise constant for each i.*

Screen foliated totally umbilical null hypersurfaces are isoparametric. In particular (future) null cone $\Lambda_0^n \subset \mathbb{R}_1^{n+1}$ are isoparametric null hypersurfaces.

2.2. **Rigged linearized operators $\widetilde{L}_r$.** The shape operator $\overset{\star}{A}$ is self-adjoint and satisfies $\overset{\star}{A}\,\xi = 0$. Its $n+1$ real valued eigenfunctions $\overset{\star}{k}_0 = 0, \overset{\star}{k}_1, \ldots, \overset{\star}{k}_n$ are the screen principal curvatures and we let $(X_0 = \xi, X_1, \ldots, X_n)$ denote a $\widetilde{g}$−orthonormal basis of eigenvector fields of $\overset{\star}{A}$, with $\operatorname{span}(X_1, \ldots, Xn) = \mathcal{S}$. For $0 \le r \le n$, the $r-th$ null mean curvature $\overset{\star}{H}_r$ of the null hypersurface with respect to the shape operator $\overset{\star}{A}$ is given by

$$\binom{n+1}{r}\overset{\star}{H}_r = \sum_{0\le i_1<\cdots<i_r\le n} \overset{\star}{k}_{i_1}\cdots\overset{\star}{k}_{i_r} \qquad \text{and} \qquad \overset{\star}{H}_0 = 1,$$

and the null hypersurface is said to be r−maximal if $\overset{\star}{H}_r = 0$ identically on M. The following notations will be in use :

$$\overset{\star}{S}_r = \sum_{0\le i_1<\cdots<i_r\le n} \overset{\star}{k}_{i_1}\cdots\overset{\star}{k}_{i_r}, \qquad \overset{\star}{S}{}_r^{\alpha} = \sum_{\substack{0\le i_1<\cdots<i_r\le n \\ i_1,\cdots,i_r\neq\alpha}} \overset{\star}{k}_{i_1}\cdots\overset{\star}{k}_{i_r}.$$

In particular $\overset{\star}{S}_0 = 1$ and $\overset{\star}{S}_1 = H$ (the null mean curvature).

For $0 \leq r \leq n+1$, the $r-th$ Newton transformation $\overset{\star}{T}_r$ with respect to the shape operator $\overset{\star}{A}$ is the End($\Gamma(TM)$) element given by

$$\overset{\star}{T}_r = \sum_{a=0}^{r} (-1)^a \ \overset{\star}{S}_a \overset{\star}{A}^{r-a} .$$

Inductively,

$$\overset{\star}{T}_0 = I \ \text{ and } \ \overset{\star}{T}_r = (-1)^r \overset{\star}{S}_r I + \overset{\star}{A} \circ \overset{\star}{T}_{r-1},$$

where I denotes the identity of $\Gamma(TM)$ and $\overset{\star}{T}_{n+1} = 0$ (follows Cayley-Hamilton's theorem). By algebraic computations, one shows the following.

Proposition 2.1 ([3])**.** .

(1) $\overset{\star}{T}_r$ *is self-adjoint and commute with* $\overset{\star}{A}$ *for any* r*;*
(2) $\overset{\star}{T}_r X_\alpha = (-1)^r \ \overset{\star}{S}_r^{\alpha} \ X_\alpha$ *(*for a fixed α);
(3) $\text{tr}(\overset{\star}{T}_r) = (-1)^r (n+1-r) \ \overset{\star}{S}_r$;
(4) $\text{tr}\left(\overset{\star}{A} \circ \overset{\star}{T}_{r-1}\right) = (-1)^{r-1} r \ \overset{\star}{S}_r$;
(5) $\text{tr}\left(\overset{\star}{A}^2 \circ \overset{\star}{T}_{r-1}\right) = (-1)^{r-1} \left(\overset{\star}{S}_1 \overset{\star}{S}_r - (r+1) \ \overset{\star}{S}_{r+1}\right)$;
(6) $\text{tr}(\overset{\star}{T}_{r-1} \circ \nabla_X \ \overset{\star}{A}) = (-1)^{r-1} X \cdot \ \overset{\star}{S}_r$.

For each Newton transformation $\overset{\star}{T}_r$, we can consider the second-order linear differential operator $\widetilde{L}_r : C^\infty(M) \to C^\infty(M)$ given by

$$\widetilde{L}_r(f) = \text{tr}\left(\overset{\star}{T}_r \circ \widetilde{\nabla}^2 f\right) \tag{2.9}$$

where $\widetilde{\nabla}^2 f := \widetilde{\nabla}\widetilde{\nabla} f$ stands for the $\widetilde{g}-$dual of the Hessian $\widetilde{Hess\ f}$ of f with respect to $\widetilde{g}$ on M. Observe that when $r = 0$, $\widetilde{L}_0 = \widetilde{\Delta}$ is nothing but the Laplacian operator on the Riemannian rigged structure $(M, \widetilde{g})$. Also, the second-order linear differential operator $\widetilde{L}_r$ defined here in (2.9) is different from $L_r(f) = \text{tr}\left(\overset{\star}{T}_r \circ \nabla(\widetilde{\nabla} f)\right)$ as defined in [5] where a hybrid use of the (projected) induced connection ∇ and the rigged Levi-Civita connection $\widetilde{\nabla}$ on $(M, \widetilde{g})$ is made. But these two connections do not coincide in general. These operators satisfy for all $f, h \in C^\infty(M)$,

$$\widetilde{L}_r(fh) = f\widetilde{L}_r(h) + h\widetilde{L}_r(f) + 2\widetilde{g}\left(\widetilde{\nabla} f, \overset{\star}{T}_r \ \widetilde{\nabla} h\right). \tag{2.10}$$

For the following orientable isometric immersion

$$\psi : M^{n+1} \longrightarrow \overline{M}_1^{n+2}(c) \subseteq \mathbb{R}^m_{1+t}$$

of the null hypersurface in $\overline{M}_1^{n+2}(c)$ where $m = n+2+c^2$ and $t = c(c-1)/2$ with $c = 1, 0, -1$, one calculates $\widetilde{L}_r$ acting on the coordinate components of the immersion ψ, i.e a function given by $\left\langle \psi, a \right\rangle$ where $a \in \mathbb{R}^m_{1+t}$ is an arbitrary fixed vector and then extend $\widetilde{L}_r$ to the $\mathbb{R}^m_t-$valued function ψ by setting

$$\widetilde{L}_r \psi = \left(\widetilde{L}_r \psi_1, \ldots, \widetilde{L}_r \psi_m\right) = \sum_{i=1}^{m} \varepsilon_i \widetilde{L}_r \langle \psi, e_i \rangle e_i,$$

where $\psi_i = \varepsilon_i\langle\psi, e_i\rangle$ and $(e_1, \ldots, e_m)$ stands for an orthonormal basis of $\mathbb{R}^m_{1+t}$ and $\varepsilon_i = \langle e_i, e_i\rangle = \pm 1$. We have [2]

$$\begin{aligned}\widetilde{L}_r\psi &= (-1)^{r+1}\Big[(n-r)\sigma\overset{\star}{S}_r + (r+1)(\lambda+1)\overset{\star}{S}_{r+1}\Big]\xi \\ &\quad + (-1)^r(r+1)\overset{\star}{S}_{r+1}\zeta + (-1)^{r+1}(n-r)c\overset{\star}{S}_r\psi, \end{aligned} \tag{2.11}$$

Also, the following holds [2, Proposition 3.3]

Proposition 2.2. *Let*

$$\psi : M^{n+1} \longrightarrow \overline{M}_1^{n+2}(c) \subseteq \mathbb{R}^m_{1+t}$$

be a isometric immersion of a null hypersurface in the Robertson-Walker space $\overline{M}_1^{n+2}(c)$ where $m = n+2+c^2$, $t = c(c-1)/2$ with $c = 1, 0, -1$, furnished with a timelike closed and conformal rigging vector field ζ. If $\lambda = \langle\zeta, \zeta\rangle$ denotes the squared length function of ζ and σ its conformal factor, Then,

$$\begin{aligned}\widetilde{L}_r^2\psi &= \Big[(r+1)(\lambda+1)\overset{\star}{S}_{r+1} + (n-r)\sigma\overset{\star}{S}_r\Big]\widetilde{\nabla}\overset{\star}{S}_{r+1} \\ &\quad + 2(-1)^r(r+1)(\lambda+1)(\overset{\star}{T}_r \circ \overset{\star}{A})\widetilde{\nabla}\overset{\star}{S}_{r+1} \\ &\quad + 2(-1)^r(n-r)\sigma(\overset{\star}{T}_r \circ \overset{\star}{A})\widetilde{\nabla}\overset{\star}{S}_r \\ &\quad + 2(-1)^r(r+1)\sigma\,\overset{\star}{T}_r\widetilde{\nabla}\overset{\star}{S}_{r+1} \\ &\quad + 2(-1)^{r+1}(n-r)c\,\overset{\star}{T}_r\widetilde{\nabla}\overset{\star}{S}_r \\ &\quad + \Lambda_r^\xi\xi + \Lambda_r^\zeta\zeta + \Lambda_r^\psi\psi; \end{aligned} \tag{2.12}$$

with Λ_r^ξ, Λ_r^ζ and Λ_r^ψ as follows :

$$\begin{aligned}\Lambda_r^\xi &= (-1)^{r+1}(r+1)(\lambda+1)\widetilde{L}_r\overset{\star}{S}_{r+1} + (-1)^{r+1}\sigma(n-r)\widetilde{L}_r\overset{\star}{S}_r \\ &\quad + (r+1)\lambda\left(\frac{1}{2}(\lambda+1)\overset{\star}{S}_1 - 2(r+1)\sigma\right)\overset{\star}{S}^2_{r+1} + c(n-r)^2\sigma\overset{\star}{S}^2_r \\ &\quad + (n-r)\left(\frac{1}{2}\lambda\sigma\overset{\star}{S}_1 + (r+1)(c\lambda - 2\sigma^2)\right)\overset{\star}{S}_r\overset{\star}{S}_{r+1} \\ &\quad + \frac{1}{2}(r+1)(r+2)\lambda(\lambda+1)\overset{\star}{S}_{r+1}\overset{\star}{S}_{r+2} \\ &\quad + \frac{1}{2}(r+2)(n-r)\lambda\sigma\overset{\star}{S}_r\overset{\star}{S}_{r+2} + 2(n-r)c\overset{\star}{S}_r(\xi\cdot\overset{\star}{S}_r) \\ &\quad - \Big[(r+1)(\lambda+1)\overset{\star}{S}_{r+1} + \sigma(n+3r+4)\overset{\star}{S}_r\Big](\xi\cdot\overset{\star}{S}_{r+1}); \end{aligned} \tag{2.13}$$

$$\Lambda_r^\zeta = (r+1)\left[(-1)^r\widetilde{L}_r\overset{\star}{S}_{r+1} + (r+1)\sigma\overset{\star}{S}^2_{r+1} - (n-r)c\overset{\star}{S}_r\overset{\star}{S}_{r+1}\right] \tag{2.14}$$

and

$$\begin{aligned}\Lambda_r^\psi &= c\Big[(-1)^{r+1}(n-r)\widetilde{L}_r\overset{\star}{S}_r + (n-r)^2c\overset{\star}{S}^2_r - (r+1)^2\lambda\overset{\star}{S}^2_{r+1} \\ &\quad - 2(r+1)(n-r)\sigma\overset{\star}{S}_r\overset{\star}{S}_{r+1} - 2(r+1)\overset{\star}{S}_r(\xi\cdot\overset{\star}{S}_{r+1})\Big]. \end{aligned} \tag{2.15}$$

Remark 2.1. *Observe that*

$$\widetilde{\nabla}\overset{\star}{S}_r = P\widetilde{\nabla}\overset{\star}{S}_r + (\xi\cdot\overset{\star}{S}_r)\xi, \quad \overset{\star}{T}_r\,\widetilde{\nabla}\,\overset{\star}{S}_r = P\left[\overset{\star}{T}_r\,\widetilde{\nabla}\,\overset{\star}{S}_r\right] + (-1)^r\,\overset{\star}{S}_r\,(\xi\cdot\overset{\star}{S}_r)\xi$$

and similar formulas for $\widetilde{\nabla}\overset{\star}{S}_{r+1}$ *and* $\overset{\star}{T}_r\widetilde{\nabla}\overset{\star}{S}_{r+1}$. *So we get the following useful equivalent formula for (2.12)*

$$\begin{aligned}\widetilde{L}_r^2\psi &= \left[(r+1)(\lambda+1)\overset{\star}{S}_{r+1}+(n-r)\sigma\overset{\star}{S}_r\right]P\widetilde{\nabla}\overset{\star}{S}_{r+1}\\ &+2(-1)^r(r+1)(\lambda+1)(\overset{\star}{T}_r\circ\overset{\star}{A})\widetilde{\nabla}\overset{\star}{S}_{r+1}\\ &+2(-1)^r(n-r)\sigma(\overset{\star}{T}_r\circ\overset{\star}{A})\widetilde{\nabla}\overset{\star}{S}_r\\ &+2(-1)^r(r+1)\sigma P\overset{\star}{T}_r\widetilde{\nabla}\overset{\star}{S}_{r+1}\\ &+2(-1)^{r+1}(n-r)cP\overset{\star}{T}_r\widetilde{\nabla}\overset{\star}{S}_r\\ &+\overset{\star}{\Lambda}_r^{\xi}\xi+\Lambda_r^{\zeta}\zeta+\Lambda_r^{\psi}\psi; \end{aligned}\tag{2.16}$$

with

$$\begin{aligned}\overset{\star}{\Lambda}_r^{\xi} &= (-1)^{r+1}(r+1)(\lambda+1)\widetilde{L}_r\overset{\star}{S}_{r+1}+(-1)^{r+1}\sigma(n-r)\widetilde{L}_r\overset{\star}{S}_r\\ &+(r+1)\lambda\left(\frac{1}{2}(\lambda+1)\overset{\star}{S}_1-2(r+1)\sigma\right)\overset{\star}{S}{}^2_{r+1}+c(n-r)^2\sigma\overset{\star}{S}{}^2_r\\ &+(n-r)\left(\frac{1}{2}\lambda\sigma\overset{\star}{S}_1+(r+1)(c\lambda-2\sigma^2)\right)\overset{\star}{S}_r\overset{\star}{S}_{r+1}\\ &+\frac{1}{2}(r+1)(r+2)\lambda(\lambda+1)\overset{\star}{S}_{r+1}\overset{\star}{S}_{r+2}\\ &+\frac{1}{2}(r+2)(n-r)\lambda\sigma\overset{\star}{S}_r\overset{\star}{S}_{r+2}-2(r+1)\sigma\overset{\star}{S}_r(\xi\cdot\overset{\star}{S}_{r+1}).\end{aligned}\tag{2.17}$$

For further use we recall the following.

Theorem 2.1. [2, Theorem 3.1]. *Let* (M^{n+1},ζ) *be a normalized null hypersurface of a Lorentzian space form* $(\overline{M}_1^{n+2}(c),\bar{g})$ *with rigged vector field* ξ *and* $\tau=0$. *Then,*

$$\xi\cdot\overset{\star}{S}_r=(-1)^{r-1}tr\left(\overset{\star}{A}{}^2\circ\overset{\star}{T}_{r-1}\right)\overset{Prop.\ 2.1\ (5)}{=}\left(\overset{\star}{S}_1\overset{\star}{S}_r-(r+1)\overset{\star}{S}_{r+1}\right).\tag{2.18}$$

Consequently, if $\overset{\star}{S}_r=0$ *for some* $r=1,...,n$, *then* $\overset{\star}{S}_k=0$ *for all* $k\geq r$.

3. $\widetilde{L_r}-1-$ TYPE NULL HYPERSURFACES IN GRW SPACETIMES

Assume $\psi:M^{n+1}\longrightarrow\overline{M}_1^{n+2}(c)\subset\mathbb{R}^m_{1+t}$ is $\widetilde{L}_r$-1-type $(0\leqslant r\leqslant n-1)$. Then $\psi-\psi_0=\psi_1$ with $\widetilde{L}_r\psi_1=\alpha\psi_1,\ (\alpha\in\mathbb{R})$. Hence, we have $\widetilde{L}_r\psi=\widetilde{L}_r\psi_1=\alpha\psi_1=\alpha(\psi-\psi_0)=\alpha\psi-\alpha\psi_0$. If we put $b=-\alpha\psi_0$, we have:

$$\widetilde{L}_r\psi=\alpha\psi+b.\tag{3.19}$$

Let $U=PU+\omega(U)\xi\in\mathfrak{X}(M)$. Taking derivative of (3.19) with respect to U leads to

$$\begin{aligned}&\left[\sigma(r+1)\overset{\star}{S}_{r+1}\omega(U)+(\lambda+1)(r+1)U\cdot\overset{\star}{S}_{r+1}+\sigma(n-r)U\cdot\overset{\star}{S}_r+(-1)^r\alpha\omega(U)\right]\xi\\ &-\left[(r+1)U\cdot\overset{\star}{S}_{r+1}\right]\zeta+c\left[(n-r)U\cdot\overset{\star}{S}_r+(r+1)\overset{\star}{S}_{r+1}\omega(U)\right]\psi\\ &-\left[(\lambda+1)(r+1)\overset{\star}{S}_{r+1}+\sigma(n-r)\overset{\star}{S}_r\right]\overset{\star}{A}(U)+\left[c(n-r)\overset{\star}{S}_r-\sigma(r+1)\overset{\star}{S}_{r+1}+(-1)^r\alpha\right]PU=0\end{aligned}\tag{3.20}$$

which is equivalent to

$$(r+1)U\cdot\overset{\star}{S}_{r+1}=0\tag{3.21}$$

$$c\left[(n-r)U\cdot\overset{\star}{S}_r+(r+1)\overset{\star}{S}_{r+1}\omega(U)\right]=0 \tag{3.22}$$

$$\sigma\left[(r+1)\overset{\star}{S}_{r+1}\omega(U)+(n-r)U\cdot\overset{\star}{S}_r\right]+(r+1)\,(\lambda+1)\,U\cdot\overset{\star}{S}_{r+1}+(-1)^r\alpha\omega(U)=0 \tag{3.23}$$

$$-\left[(\lambda+1)(r+1)\overset{\star}{S}_{r+1}+\sigma(n-r)\overset{\star}{S}_r\right]\overset{\star}{A}(U)+\left[c(n-r)\overset{\star}{S}_r-\sigma(r+1)\overset{\star}{S}_{r+1}+(-1)^r\alpha\right]PU=0 \tag{3.24}$$

Furthermore, combining (3.19), (2.11) and the following decomposition

$$b=Pb^{\top}+\langle b,\zeta-\lambda\xi\rangle\xi+\langle b,\xi\rangle\zeta+c\langle b,\psi\rangle\psi,$$

lead to

$$(-1)^{r+1}\left[(\lambda+1)\,(r+1)\overset{\star}{S}_{r+1}+\sigma(n-r)\overset{\star}{S}_r\right]=\langle b,\zeta-\lambda\xi\rangle \tag{3.25}$$

$$(-1)^r\,(r+1)\overset{\star}{S}_{r+1}=\langle b,\xi\rangle \tag{3.26}$$

$$(-1)^{r+1}\,c(n-r)\overset{\star}{S}_r=\alpha+c\langle b,\psi\rangle \tag{3.27}$$

$$Pb^{\top}=0 \tag{3.28}$$

We discuss separately the cases when $c\in\{-1,+1\}$ and $c=0$.

Case: $c\in\{-1,+1\}$

Equations (3.22) and (3.23) imply $\alpha=0$ and $b=-\alpha\psi_0=0$. Substituting $\alpha=0$ and $b=0$ into Eqs. (3.26) and (3.27) yields for $0\leq r<n$ that $\overset{\star}{S}_r=0$ and $\overset{\star}{S}_{r+1}=0$. Making use of Theorem 2.1 we can thus state the following.

Theorem 3.1. *Let $\psi:M^{n+1}\longrightarrow\overline{M}_1^{n+2}(c)\subset\mathbb{R}^m_{1+t}$ be a connected isometric immersion of a null hypersurface in a GRW spacetime $\overline{M}_1^{n+2}(\pm1)$, endowed with a timelike closed and conformal rigging vector field ζ. Then, M is $\widetilde{L}_r$-1-type $(0\leq r<n)$ if and only if $\overset{\star}{S}_r=0$.*

Example 3.1. *Let $n\geq m\geq 2$ be integers. Consider*

$$M=\{x\in\mathbb{L}^{n+3}\mid -x_0^2+x_1^2+\cdots+x_{m+1}^2=0,\quad x_{m+2}^2+\cdots+x_{n+2}^2=1\}\cap\{x_0>0\}.$$

It is easy to see that $M=\Lambda_0^{m+1}\times\mathbb{S}^{n-m}$ is a null hypersurface of the De Sitter spacetime $\mathbb{S}_1^{n+2}$ given by the product of the lightcone Λ_0^{m+1} of dimension $m+1$ with the $n-m$ standard sphere $\mathbb{S}^{n-m}$ (a null cone torus). A timelike closed and conformal rigging for M is given by

$$\zeta=\partial_0+x_0x,$$

with (null) rigged vector field

$$\xi=-\frac{1}{x_0}\cdot\Big(x_0,x_1,\ldots,x_{m+1},0,\ldots,0\Big).$$

Then the shape operator is

$$\overset{\star}{A}\simeq\left[\begin{array}{c|c}0\quad\cdots\quad\cdots\quad 0&\\ \vdots\quad\frac{1}{x_0}I_m\quad\quad 0&\\ \hline \vdots\quad 0\quad\quad 0_{n-m}&\\ 0&\end{array}\right],$$

and we get that

$$\overset{\star}{H}_r=\begin{cases}\binom{n+1}{r}^{-1}\binom{m}{r}\cdot\dfrac{1}{(x_0)^r} & \text{if} \qquad 0\leq r\leq m\\ \\ 0 & \text{if} \quad m+1\leq r\leq n+1\end{cases} \tag{3.29}$$

Hence, the null cone torus $M=\Lambda_0^{m+1}\times\mathbb{S}^{n-m}$ *is* $\widetilde{L}_r-1-$*type for* $m+1\leq r\leq n+1$.

Case: $c=0$

When $c=0$, equation (3.27) implies $\alpha=0$ and $b=0$. Thus, equation (3.26) gives $\overset{\star}{S}_{r+1}=0$ and, for $0\leq r<n$, equation (3.25) implies $\sigma=0$ or $\overset{\star}{S}_r$. It follows that ($\sigma|_M=0$ and $\overset{\star}{S}_{r+1}=0$) or $\overset{\star}{S}_r=0$. Since by Theorem 2.1, $\overset{\star}{S}_r=0$ implies $\overset{\star}{S}_{r+1}=0$, above condition is equivalent to $\overset{\star}{S}_{r+1}=0$ and ($\overset{\star}{S}_r=0$ or $\sigma|_M=0$). Thus, we can state the following:

Theorem 3.2. *Let* $\psi:M^{n+1}\longrightarrow\overline{M}_1^{n+2}(0)\subset\mathbb{R}^m_{1+t}$ *be a connected isometric immersion of a null hypersurface in GRW spacetime* $\overline{M}_1^{n+2}(0)$*, furnished with a timelike closed and conformal rigging vector field* ζ *with conformal factor* σ*. Then,* M *is* $\widetilde{L}_r$*-1-type* $(0\leqslant r\leqslant n-1)$ *if and only if* $\overset{\star}{S}_{r+1}=0$ *and* ($\overset{\star}{S}_r=0$ *or* $\sigma|_M=0$).

Example 3.2. *Let* $m\geqslant 1$ *be an integer and consider the in the Minkowski spacetime* $\mathbb{R}_1^{2m+2}$ *with coordinates* $(t,x_1,\ldots,x_{2m+1})$ *the null hypersurface*

$$\Sigma_m=\left\{(t,x_1,\ldots,x_{2m+1})\in\mathbb{R}_1^{2m+2}\mid t=-\sqrt{x_{m+1}^2+\cdots+x_{2m+1}^2}<0\right\}.$$

It is easy to see that Σ_m *is a null hypersurface, as the gradient of the defining function* $u=t+\sqrt{x_{m+1}^2+\cdots+x_{2m+1}^2}$ *is a null vector field. A rigging for* Σ_m *is the timelike closed and conformal vector field* $\zeta=\partial_t$ *for which* σ *vanishes identically. The associated rigged vector field (null generator normalized by* $g(\xi,\zeta)=1$*) is*

$$\xi=-\partial_t+\sum_{k=m+1}^{2m+1}\frac{x_k}{R}\partial_{x_k},\quad \text{where } R=\sqrt{x_{m+1}^2+\cdots+x_{2m+1}^2}.$$

Then, with respect to a screen distribution $S=\operatorname{span}\{\partial_{x_1},\ldots,\partial_{x_m}\}\oplus T\mathbb{S}^{m-1}$*, the shape operator takes the form*

$$\overset{\star}{A}\simeq\left[\begin{array}{c|c}0_m & 0\\ \hline 0 & -\frac{1}{R}I_{m+1}\end{array}\right],$$

and we obtain that the r*-th mean curvature is*

$$\overset{\star}{H}_r=\begin{cases}\binom{m}{r}^{-1}\left(-\dfrac{1}{R}\right)^r & \text{if } 0\leq r\leq m+1,\\ 0 & \text{if } m+1<r\leq 2m+1.\end{cases}$$

Hence, Σ_m *is* $\widetilde{L}_r-1-$*type for* $m+1<r\leq 2m+1$ *since* $\sigma\equiv 0$ *and* $\overset{\star}{S}_r=0$ *for* $m+1<r\leq 2m+1$.

Corollary 3.1. *Let $\psi : M^{n+1} \longrightarrow \overline{M}_1^{n+2}(0) \subset \mathbb{R}^m_{1+t}$ denote a connected isometric immersion of a null hypersurface in a Generalized Robertson-Walker (GRW) spacetime $\overline{M}_1^{n+2}(0)$, endowed with a timelike closed and conformal rigging vector field ζ. If M is of $\widetilde{L}_r$-1-type $(0 \leqslant r \leqslant n-1)$, then at least one of the following conditions holds:*

(1) $\overset{\star}{S}_r = 0$.
(2) $\sigma = \overset{\star}{S}_{r+1} = 0$.

4. $\widetilde{L_r} - 2-$ type null hypersurfaces in GRW spacetimes

Let $\psi : M^{n+1} \longrightarrow \overline{M}_1^{n+2}(c) \subset \mathbb{R}^m_{1+t}$ be $\widetilde{L}_r$-2-type $(0 \leqslant r \leqslant n-1)$. Then $\psi - \psi_0 = \psi_1 + \psi_2$ with $\widetilde{L}_r\psi_1 = \lambda_1\psi_1$ and $\widetilde{L}_r\psi_2 = \lambda_2\psi_2$. We have

$$\widetilde{L}_r^2\psi = (\lambda_1 + \lambda_2)\,\widetilde{L}_r\psi - \lambda_1\lambda_2\,(\psi - \psi_0)\,. \tag{4.30}$$

Therefore, (2.11) and Proposition 2.2 in (4.30) provide

$$(-1)^{r+1}\,(\lambda_1 + \lambda_2)\left[(\lambda+1)\,(r+1)\overset{\star}{S}_{r+1} + \sigma(n-r)\overset{\star}{S}_r\right] + \lambda_1\lambda_2\langle\psi_0, \zeta - \lambda\xi\rangle = \overset{\star}{\Lambda}{}_r^{\xi} \tag{4.31}$$

$$(-1)^{r}\,(\lambda_1 + \lambda_2)\,(r+1)\overset{\star}{S}_{r+1} + \lambda_1\lambda_2\langle\psi_0, \xi\rangle = \Lambda_r^{\zeta} \tag{4.32}$$

$$(-1)^{r}\,(\lambda_1 + \lambda_2)\,c(n-r)\overset{\star}{S}_r - \lambda_1\lambda_2 + c\lambda_1\lambda_2\langle\psi_0, \psi\rangle = \Lambda_r^{\psi} \tag{4.33}$$

$$\lambda_1\lambda_2 \mathrm{P}\psi_0^{\top} = \mathrm{P}\widetilde{L_r}^2\psi \tag{4.34}$$

Consider $\overset{\star}{S}_r$ to be a non-zero constant and assume first that $c \neq 0$. It follows from Theorem 2.1 that $\xi \cdot \overset{\star}{S}_r = 0 = \overset{\star}{S}_1\overset{\star}{S}_r - (r+1)\overset{\star}{S}_{r+1}$, which implies $\overset{\star}{S}_{r+1} = \dfrac{\overset{\star}{S}_r}{r+1}\overset{\star}{S}_1$. Thus, $\widetilde{\nabla}\overset{\star}{S}_{r+1} = \dfrac{\overset{\star}{S}_r}{r+1}\widetilde{\nabla}\overset{\star}{S}_1$. Moreover, $\xi\cdot\overset{\star}{S}_{r+1} = \dfrac{\overset{\star}{S}_r}{(r+1)}\left|\overset{\star}{A}\right|^2$ and we get $\overset{\star}{S}_{r+2} = \dfrac{2}{(r+1)(r+2)}\overset{\star}{S}_2\overset{\star}{S}_r$. Therefore, $\widetilde{\nabla}\overset{\star}{S}_{r+2} = \dfrac{2\overset{\star}{S}_r}{(r+1)(r+2)}\widetilde{\nabla}\overset{\star}{S}_2$. It can also be shown that

$$\widetilde{\nabla}\left(\xi \cdot \overset{\star}{S}_{r+1}\right) = \frac{2\overset{\star}{S}_r}{(r+1)}\left(\overset{\star}{S}_1\widetilde{\nabla}\overset{\star}{S}_1 - \widetilde{\nabla}\overset{\star}{S}_2\right).$$

Consequently,

$$P\widetilde{\nabla}\overset{\star}{S}_{r+1} = \frac{\overset{\star}{S}_r}{r+1}P\widetilde{\nabla}\overset{\star}{S}_1 \tag{4.35}$$

and

$$P\widetilde{\nabla}\left(\xi \cdot \overset{\star}{S}_{r+1}\right) = \frac{2\overset{\star}{S}_r}{(r+1)}\left(\overset{\star}{S}_1 P\widetilde{\nabla}\overset{\star}{S}_1 - P\widetilde{\nabla}\overset{\star}{S}_2\right) \tag{4.36}$$

Besides, combining equations (4.31), (4.32), and (4.33), we have:

$$(\lambda+1)\left[\lambda_1\lambda_2\,\langle\psi_0, \xi\rangle - \Lambda_r^{\zeta}\right] + \sigma\left[c\Lambda_r^{\psi} + c\lambda_1\lambda_2 - \lambda_1\lambda_2\,\langle\psi_0, \psi\rangle\right] + \lambda_1\lambda_2\,\langle\psi_0, \zeta - \lambda\xi\rangle = \overset{\star}{\Lambda}{}_r^{\xi}, \tag{4.37}$$

and this, after reduction provides

$$\lambda_1\lambda_2\langle\psi_0,\xi\rangle - \sigma\overset{\star}{S}_1^2\overset{\star}{S}_r^2 + c(n-r)\overset{\star}{S}_r^2\overset{\star}{S}_1 + c\sigma\lambda_1\lambda_2 - \sigma\lambda_1\lambda_2\langle\psi_0,\psi\rangle + \lambda_1\lambda_2\langle\psi_0,\zeta\rangle$$
$$= \frac{3}{2(r+1)}\overset{\star}{S}_r^2\left(\overset{\star}{S}_1^3 + \overset{\star}{S}_1\overset{\star}{S}_2\right) + \frac{3(n-r)}{2(r+1)}\overset{\star}{S}_r^2\left(\lambda\sigma\overset{\star}{S}_1^2 + \lambda\sigma\overset{\star}{S}_2\right).$$

Now, we prove the following:

Theorem 4.1. *Let $\psi : M^{n+1} \longrightarrow \overline{M}_1^{n+2}(c) \subset \mathbb{R}^m_{1+t}$ be an isometric immersion of a null hypersurface into a generalized Robertson-Walker spacetime $\overline{M}_1^{n+2}(c)$, where $m = n+2+c^2$, $t = \frac{1}{2}c(c-1)$ with $c = \pm 1$, endowed with a closed and conformal rigging field ζ. Suppose $\overset{\star}{S}_2$ non zero constant. For $r \in \{0,1,2\}$, the $\widetilde{L_r} - 2-$ type property implies that the null hypersurface is isoparametric.*

Proof. Consider the relation (4.38) with $r = 2$ in which $\overset{\star}{S}_2$ is a non-zero constant. Then,

$$\lambda_1\lambda_2\langle\psi_0,\xi\rangle - \sigma\overset{\star}{S}_1^2\overset{\star}{S}_2^2 + c(n-2)\overset{\star}{S}_2^2\overset{\star}{S}_1 + c\sigma\lambda_1\lambda_2 - \sigma\lambda_1\lambda_2\langle\psi_0,\psi\rangle + \lambda_1\lambda_2\langle\psi_0,\zeta\rangle$$
$$= \frac{1}{2}\overset{\star}{S}_2^2\left(\overset{\star}{S}_1^3 + \overset{\star}{S}_1\overset{\star}{S}_2\right) + \frac{(n-2)}{2}\overset{\star}{S}_2^2\lambda\sigma\left(\overset{\star}{S}_1^2 + \overset{\star}{S}_2\right). \tag{4.38}$$

By differentiating the relation (4.38) three times with respect to ξ noting that

$$\xi\cdot\left|\overset{\star}{A}\right|^2 = 2\overset{\star}{S}_1\left|\overset{\star}{A}\right|^2 \text{ and } \xi\cdot\overset{\star}{S}_1 = \left|\overset{\star}{A}\right|^2,$$

and then repeatedly differentiationg with respect to $X \in \mathcal{S}^\zeta$, we obtain:

$$X\cdot\overset{\star}{S}_1 = 0 \quad \text{or} \quad \overset{\star}{S}_2 = 0 \quad \text{or} \quad \lambda = 0. \tag{4.39}$$

But, $\overset{\star}{S}_2 \neq 0$ and $\lambda < 0$ since ζ is timelike. It follows that $\overset{\star}{S}_1$ is (screen) leafwise constant. Observe that under the condition $\overset{\star}{S}_2$ is a non zero constant, for each $k \in \mathbb{N}^\star$ the following holds.

$$\begin{cases} \overset{\star}{S}_{2k} &= \dfrac{\left(2\overset{\star}{S}_2\right)^k}{(2k)!}, \\ \widetilde{\nabla}\overset{\star}{S}_{2k+1} &= \dfrac{1}{2k+1}\overset{\star}{S}_{2k}\widetilde{\nabla}\overset{\star}{S}_1 \end{cases} \tag{4.40}$$

which implies

$$P\widetilde{\nabla}\overset{\star}{S}_{2k} = 0 \text{ and } P\widetilde{\nabla}\overset{\star}{S}_{2k+1} = \frac{1}{2k+1}\overset{\star}{S}_{2k}P\widetilde{\nabla}\overset{\star}{S}_1 = 0.$$

It follows that for all k, $\overset{\star}{S}_k$ is (screen) leafwise constant and this is equivalent to saying that the principal curvatures are also (screen) leafwise constant. We conclude that M is isoparametric.

The proof for $r = 1$ or $r = 0$ is exactly the same. □

Theorem 4.2. *Let $\psi : M^{n+1} \longrightarrow \overline{M}_1^{n+2}(c) \subset \mathbb{R}^m_{1+t}$ be a connected isometric immersion of a null hypersurface in GRW spacetime $\overline{M}_1^{n+2}(c)$ $(c = \pm 1)$, furnished with a timelike closed and conformal rigging vector field ζ. Assume that $\overset{\star}{S}_r$ and $\overset{\star}{S}_2$ are non-zero constant*

Then M is $\widetilde{L}_r$-null-2-type $(0 \leqslant r \leqslant n-1)$ if and only if M is isoparametric.

Proof. Since $\lambda_1 = 0$ or $\lambda_2 = 0$, equation (4.38) reduces to:

$$-\sigma \overset{\star}{S}_1^2 \overset{\star}{S}_r^2 + c(n-r)\overset{\star}{S}_r^2 \overset{\star}{S}_1 = \frac{3}{2(r+1)}\ \overset{\star}{S}_r^2 \left(\overset{\star}{S}_1^3 + \overset{\star}{S}_1 \overset{\star}{S}_2\right) + \frac{3(n-r)}{2(r+1)}\ \overset{\star}{S}_r^2\ \lambda\sigma \left(\overset{\star}{S}_1^2 + \overset{\star}{S}_2\right) \quad (4.41)$$

Repeatedly differentiating (4.41) with respect to a generic $X \in \mathcal{S}^\zeta$ leads to $X \cdot \overset{\star}{S}_1 = 0$ and we see that $\overset{\star}{S}_1$ is (screen) leafwise constant. Use ((4.40), to conclude that $\overset{\star}{S}_k$ is (screen) leafwise constant for all k and M is isoparametric. □

Example 4.1. *Let $\overline{M} = \mathbb{R} \times_{e^t} \mathbb{R}^{n+1}$ with metric $\overline{g} = -dt^2 + e^{2t}\left(\sum_{i=1}^{n+1}(dx^i)^2\right)$. This is a GRW space with constant curvature $c = 1$. Consider*

$$L = \left\{x^1 = e^{-t}\right\}.$$

Define the function $\varphi = x^1 - e^{-t}$, where. We see that $|\nabla\varphi|^2 = 0$ and L is a null hypersurface. Then take the rigging vector field to be the timelike closed and conformal vector field $\zeta = \partial_t$. The associated rigged vector field is given by $\xi = -\partial_t + e^{-t}\partial_{x^1}$. Also, for each $p \in M$ the tangent space is $T_pL = Span\{\xi = \partial_t + e^{-t}\partial_{x^1}, \partial_{x^2}, \ldots, \partial_{x^{n+1}}\}$ and we have for all $i = 2, \ldots, n+1$,

$$\overline{\nabla}_{\partial_{x^i}}\xi = \nabla_{\partial_{x^i}}\xi = -\partial_{x^i} = -\overset{\star}{A}(\partial_{x^i}).$$

Since $\mathcal{S}^\zeta = Span\{\partial_{x^2}, \ldots, \partial_{x^{n+1}}\}$, this implies that for all $U \in \mathcal{S}^\zeta$, $\overset{\star}{A}(U) = U$ from which the conditions of Theorem 4.2 are fulfilled and L is $\widetilde{L}_r$-null-2-type $(0 \leqslant r \leqslant n-1)$.

Let us now deal with the case where $c = 0$ which by Eqs. (4.33) and (2.15) imply $\lambda_1\lambda_2 = 0$. Without loss of generality, assume $\lambda_1 = 0$. Then, combining equations (4.31), (4.32) and (4.33) yields:

$$\begin{aligned}(-1)^{r+1}\,\lambda_2\sigma(n-r)\ \overset{\star}{S}_r \;=\; & \left[-\lambda\sigma + \frac{1}{2(r+1)}\lambda\sigma(n-r) - 2\sigma^2(n-r) - \sigma\right]\ \overset{\star}{S}_r\ \overset{\star}{S}_1^2 \\ & + \frac{1}{2(r+1)}\lambda(\lambda+1)\ \overset{\star}{S}_r^2\ \overset{\star}{S}_1^3 + \frac{1}{r+1}\lambda(\lambda+1)\overset{\star}{S}_1\ \overset{\star}{S}_r^2\ \overset{\star}{S}_2 \\ & + \frac{\lambda\sigma}{r+1}(n-r)\ \overset{\star}{S}_r^2\ \overset{\star}{S}_2 + 4\sigma\ \overset{\star}{S}_r^2\ \overset{\star}{S}_2 \end{aligned} \quad (4.42)$$

Now, consider $\overset{\star}{S}_2$ to be non zero constant. By differentiating (4.42) (repeatedly) with respect to $X \in \mathcal{S}^\zeta$, it follows that $\lambda = 0$, $\lambda = -1$ or $X \cdot \overset{\star}{S}_1 = 0$. But again, $\lambda < 0$ as ζ is timelike. In fact, both cases $\lambda = -1$ or $X \cdot \overset{\star}{S}_1 = 0$ leads to M is isoparametric. Indeed, for $\lambda = -1$, we obtain

$$\begin{aligned}(-1)^{r+1}\,\lambda_2\sigma(n-r)\ \overset{\star}{S}_r \;=\; & \left[-\frac{1}{2(r+1)}\sigma(n-r) - 2\sigma^2(n-r)\right]\ \overset{\star}{S}_r\ \overset{\star}{S}_1^2 \\ & - \frac{\sigma}{r+1}(n-r)\ \overset{\star}{S}_r^2\ \overset{\star}{S}_2 + 4\sigma\ \overset{\star}{S}_r^2\ \overset{\star}{S}_2. \end{aligned} \quad (4.43)$$

We conclude that $\overset{\star}{S}_1$ is screen lifewise constant as it is solution of a second order algebraic equation with (screen) leafwise constant coefficients. Now, using again (4.40) under the condition that $\overset{\star}{S}_2$ is leafwise constant leads to isoparametry as all $\overset{\star}{S}_r$ are leafwise constant.

Therefore, we can state the following.

Theorem 4.3. *Let $\psi : M^{n+1} \longrightarrow \mathbb{R}_1^{n+2}$ be a connected isometric immersion of a null hypersurface in the Minkowski space $\mathbb{R}_1^{n+2}$, furnished with a timelike closed and conformal rigging vector field ζ. Assume that $\overset{\star}{S}_r$ and $\overset{\star}{S}_2$ are non-zero constant.*

Then M is $\widetilde{L}_r$-2-type $(0 \leqslant r \leqslant n-1)$ if and only if M is isoparametric.

References

[1] Alias, L. J., & Gurbuz, N. (2006). An extension of Takahashi theorem for the linearized operator of the higher order mean curvature. *Geometriae Dedicata*, *121*, 113–127.

[2] Atindogbe, C. (2025). $\widetilde{L}_r$-biharmonic null hypersurfaces in generalized Robertson–Walker spacetimes. *International Journal of Maps in Mathematics*, *8*(2), 717–750.

[3] Atindogbe, C., & Fotsing Tetsing, H. (2015). Newton transformations on null hypersurfaces. *Communications in Mathematics*, *23*, 57–83.

[4] Atindogbe, C., & Olea, B. (2022). Conformal vector fields and null hypersurfaces. *Results in Mathematics*, *77*, Article 129.

[5] Fotsing Tetsing, H., Atindogbe, C., & Ngakeu, F. (2023). Normalized null hypersurfaces in the Lorentz–Minkowski space satisfying $L_r x = Ux + b$. *Tamkang Journal of Mathematics*, *54*(4), 353–378. https://doi.org/10.5556/j.tkjm.54.2023.4851

[6] Chen, B.-Y. (1984). *Total mean curvature and submanifolds of finite type* (Series in Pure Mathematics, Vol. 1). Singapore: World Scientific.

[7] Chen, B.-Y. (2013). Riemannian submanifolds: A survey. *arXiv preprint arXiv:1307.1875*. https://doi.org/10.48550/arXiv.1307.1875

[8] Duggal, K. L., & Bejancu, A. (1996). *Lightlike submanifolds of semi-Riemannian manifolds and applications* (Vol. 364). Boston: Kluwer Academic.

[9] Duggal, K. L., & Sahin, B. (2010). *Differential geometry of lightlike submanifolds*. Basel: Birkhäuser.

[10] Gutierrez, M., & Olea, B. (2021). The rigging technique for null hypersurfaces. *Axioms*, *10*, Article 284. https://doi.org/10.3390/axioms10040284

[11] Lucas, P., & Ramírez-Ospina, H.-F. (2015). L_k-2-type hypersurfaces in hyperbolic spaces. *Taiwanese Journal of Mathematics*, *19*. https://doi.org/10.11650/tjm.19.2015.4603

[12] Navarro, M., Palmas, O., & Solis, D. A. (2018). Null screen isoparametric hypersurfaces in Lorentzian space forms. *Mediterranean Journal of Mathematics*, *15*, Article 215.

[13] Palmas, O. (2021). Null hypersurfaces with screen parallel shape operator. *Mediterranean Journal of Mathematics*, *18*, Article 133. https://doi.org/10.1007/s00009-021-01777-7

[14] Sánchez, M. (1999). On the geometry of generalized Robertson–Walker spacetimes: Curvature and Killing fields. *Journal of Geometry and Physics*, *31*, 1–15.

(E. Adedemi, C. Atindogbé and R. Hounnonkpè) University of Abomey-Calavi (UAC), Faculty of Sciences and Technologies (FAST), Department of Mathematics, 01BP 4521, Cotonou, Benin

CALCULATION

Volume ***2****, Issue* ***1****, 2026, Pages:****26–33***

E-ISSN: 3062–2107

www.simadp.com/calculation

A COMPUTATIONAL BENCHMARK OF STANDARDIZED LATTICE-BASED POST-QUANTUM SIGNATURE SCHEMES

MELIKE KARATAY *

Abstract. This article provides an expanded computational evaluation of three standardized lattice-based post-quantum signature schemes—ML-DSA-44, ML-DSA-65 and Falcon-512—using reference implementations from the Open Quantum Safe (liboqs) project. Unlike prior benchmarking efforts that rely on optimized implementations or hardware-specific tuning, this work focuses on reproducible baseline performance on a conventional CPU platform. We measure key generation, signing and verification times across 5,000 iterations and analyze the effect of message length on signing cost. Results confirm that ML-DSA variants achieve significantly faster signing and key generation, whereas Falcon-512 produces substantially smaller keys and signatures. The study further highlights the computational dominance of lattice operations over hashing, explaining the weak dependence of signing cost on message size. These findings aim to support system architects evaluating the practical feasibility of standardized post-quantum signature algorithms.

Keywords: Post-quantum cryptography, Lattice-based signatures, Performance evaluation

2020 Mathematics Subject Classification: 94A60, 68P25.

1. Introduction

The anticipated emergence of large-scale quantum computers poses a fundamental threat to classical public-key cryptosystems whose security relies on the presumed hardness of integer factorization and discrete logarithms. In response, substantial global effort has been devoted to the development of post-quantum cryptography (PQC), aiming to design cryptographic primitives that remain secure against both classical and quantum adversaries. Among the candidate families explored during the NIST Post-Quantum Cryptography Standardization Project [4], lattice-based cryptography has emerged as the most prominent due to its strong worst-case to average-case reductions [1], conceptual simplicity, and highly efficient algebraic structure [3].

Digital signature schemes constitute one of the central components of the PQC transition. ML-DSA, formerly known as CRYSTALS–Dilithium, was selected by NIST as the primary

Received: 2025.10.17 *Revised: 2025.12.16* *Accepted: 2025.12.22*

* Corresponding author

Melike Karatay ⋄ melike.karatay@fbu.edu.tr ⋄ https://orcid.org/0000-0001-6941-4752

post-quantum digital signature standard [4, 5]. ML-DSA relies on module-lattice constructions and the Fiat–Shamir-with-Abort transformation, achieving a favorable balance between security, determinism, and implementation simplicity. Falcon, another lattice-based signature scheme, was also advanced by NIST due to its compact keys and signatures and its mathematically elegant use of Fourier-based Gaussian sampling [6]. These schemes represent two distinct design philosophies within lattice-based cryptography, making their comparative evaluation both practically and theoretically significant.

A considerable body of benchmark literature exists for lattice-based signatures. Highly optimized implementations are included in the SUPERCOP benchmarking suite [9], the PQClean project provides portable and optimized CPU backends [10], and numerous studies evaluate performance on ARM microcontrollers [11], vectorized x86-64 architectures exploiting AVX2/AVX-512 instruction sets [12], or hardware-accelerated co-processors. While these studies offer valuable insights, they do not necessarily reflect the default, platform-neutral performance of unoptimized reference implementations. Reference implementations emphasize clarity and correctness over speed and therefore constitute a reproducible baseline, independent of platform-specific tuning and unavailable hardware features.

This motivates the present work. We perform a systematic, reproducible benchmark of ML-DSA-44, ML-DSA-65, and Falcon-512 using their unmodified reference C implementations from the Open Quantum Safe (liboqs) project. By avoiding compiler-dependent and architecture-dependent optimizations, our analysis isolates the inherent computational characteristics of each scheme. We further examine the influence of message length on signing cost and relate the results to the internal structure of the signing algorithms. In particular, previous studies show that lattice operations overwhelmingly dominate runtime, while hashing (e.g., SHAKE256) contributes only marginal overhead [8, 7]. Our results empirically confirm this behavior.

The contributions of this work are:

- A reproducible, platform-neutral performance benchmark of standardized lattice-based signature schemes using only reference implementations.
- An analysis of the effect of message size on signing time, with theoretical justification rooted in the structure of lattice arithmetic and hashing.
- A comparative discussion situating the results within the broader PQC benchmarking literature, highlighting implications for system architects and protocol designers.

This expanded analysis strengthens the empirical understanding of the standardized post-quantum signature landscape and provides actionable insights for researchers and practitioners preparing for PQC deployment.

2. Preliminaries

Lattice-based cryptography provides the foundation for several post-quantum signature schemes standardized or recommended by NIST. Its security relies on well-studied reductions from worst-case to average-case, particularly those associated with the Learning With Errors (LWE) problem and its structured variants such as Module-LWE and Module-SIS [1, 3]. These assumptions allow for the construction of efficient signature algorithms whose security proofs are rooted in hardness results from lattice theory.

ML-DSA, the primary NIST-selected post-quantum signature standard [4, 5], employs module lattices to construct a Fiat–Shamir with Aborts signature system. Its design emphasizes determinism, simplicity, and implementation clarity. At a high level, ML-DSA replaces Gaussian sampling with uniformly random sampling followed by rejection sampling, making it easier to implement securely while maintaining strong theoretical guaranties. The parameter sets ML-DSA-44 and ML-DSA-65 correspond to the former Dilithium-II and Dilithium-III security levels.

Falcon, in contrast, is built upon the NTRU lattice structure and employs fast Fourier sampling to generate lattice Gaussian samples [6]. This enables Falcon to achieve significantly smaller public keys and signatures, but at the cost of more computationally expensive key generation and signing operations. The complexity arises from the need for numerically stable discrete Gaussian sampling, a problem that has been extensively analyzed in the lattice-cryptography literature [7].

Hashing also plays a crucial role in lattice-based signatures. Both ML-DSA and Falcon use variants of SHAKE (SHAKE-128 or SHAKE-256) as part of their signing procedures, either for message compression or challenge generation [2]. Since hashing cost grows linearly with message length while lattice operations dominate computational complexity, the hashing component typically contributes only a small fraction of total signing time [8]. This explains why, in practice, signing performance is largely insensitive to message length—a behavior confirmed in Section 3.

All schemes tested in this study were benchmarked using their reference implementations from the Open Quantum Safe (liboqs) project [10]. Reference implementations prioritize portability, clarity, and standard compliance rather than speed. As a result, they provide a reproducible baseline for comparing algorithms without the confounding influence of architecture-dependent optimizations such as AVX2/AVX-512 vectorization [9, 12]. This makes them particularly suitable for evaluating the intrinsic computational characteristics of standardized post-quantum signatures.

2.1. **Experimental Setup.** All experiments in this work were performed on a workstation equipped with an **Intel Core i7-1165G7** processor (11th generation, 4 cores, 8 threads, base frequency 2.8 GHz, maximum turbo frequency 4.7 GHz) with full **AVX2** support. The system was configured with **32 GB RAM** and running **Ubuntu 24.04.1 LTS (64-bit)**. The detailed specification of the processor is essential because lattice-based cryptography is highly sensitive to vector instruction sets and microarchitectural differences [12, 11]. Specifying the exact model ensures reproducibility, as the runtime of lattice multiplications, NTT operations, and Gaussian sampling can vary significantly across CPU generations.

All implementations were compiled using **GCC 14.2** with the `-O3` optimization flag enabled. GCC 14 is a mature and stable compiler branch, and provides reliable support for the C implementations of liboqs and its post-quantum algorithm modules. No architecture-specific optimizations (e.g., `-march=native`, AVX-512 extensions, or handcrafted intrinsics) were enabled in order to preserve portability and ensure that the measurements reflect the behavior of the unoptimized reference implementations.

All signature schemes in this study were obtained from the **Open Quantum Safe (liboqs) reference implementation** [10]. The library was compiled from source against the

system's **OpenSSL 3.x** installation using its default reference configuration. No vendor-specific patches, no deterministic or randomized Gaussian sampling accelerations, and no fast polynomial multiplication overrides were applied.

Timing measurements were performed using `clock_gettime()` with the `CLOCK_MONOTONIC` flag. For each scheme, **5,000 iterations** of key generation, signing, and verification were executed, and the average runtime per operation was recorded. This iteration count follows common practice in PQC benchmarking literature to eliminate noise from short-lived operations [9, 11].

Benchmarking was performed using the baseline, non-optimized reference implementations to ensure reproducibility and consistency with the NIST PQC standardization documents. Timing measurements were obtained using clock_gettime() with CLOCK_MONOTONIC, and each operation (key generation, signing, verification) was averaged over 5,000 iterations.

3. Experimental Results

This section presents the empirical evaluation of ML-DSA-44, ML-DSA-65, and Falcon-512 using the reference implementations from the Open Quantum Safe (liboqs) framework. All results reflect the performance of non-optimized, platform-neutral implementations and provide a baseline for reproducible comparison, in contrast to prior studies relying on heavily optimized code paths [9, 10, 12]. Each operation was executed 5,000 times, and average runtimes were recorded.

3.1. **Memory Footprint.** Table 3.1 reports public key, secret key, and signature sizes for each scheme. These values are fixed parameters determined by the underlying lattice constructions. Falcon-512 achieves substantially smaller keys and signatures, a known consequence of its NTRU-based structure and its compact sampling techniques [6]. By comparison, ML-DSA variants feature larger public and secret keys due to their module-lattice structure and rejection-based signing design [5].

Table 3.1. Key and signature sizes (bytes)

Algorithm	Public Key	Secret Key	Signature
ML-DSA-44	1312	2460	2420
ML-DSA-65	1952	4032	3309
Falcon-512	897	1281	752

The differences observed here align with existing literature: Falcon is typically selected for size-constrained environments (IoT devices, embedded platforms), whereas ML-DSA is often preferred in high-throughput server environments where bandwidth is not the primary limitation [11, 8].

3.2. **Key Generation, Signing, and Verification Times.** Table 3.2 summarizes the average runtime (ms/op) for key generation, signing, and verification using 32-byte messages. The results indicate that ML-DSA-44 exhibits the fastest key generation and signing performance. ML-DSA-65, which targets a higher NIST security level, remains computationally efficient despite its increased parameter sizes. Falcon-512, however, presents a significantly different performance profile: **key generation is nearly two orders of magnitude slower**.

TABLE 3.2. Average runtime (ms/op) for 32-byte messages

Algorithm	KeyGen	Sign	Verify
ML-DSA-44	0.03075	0.08019	0.02803
ML-DSA-65	0.04961	0.12638	0.04743
Falcon-512	6.74992	0.22014	0.04794

This observation is consistent with prior reports documenting the high computational cost of its floating-point Gaussian sampling algorithm [6, 8]. Gaussian sampling dominates Falcon's key generation, whereas ML-DSA relies on more lightweight polynomial operations and deterministic rejection sampling.

Verification performance is relatively consistent across schemes, with ML-DSA variants achieving marginally faster verification than Falcon, in line with prior benchmark studies [9, 10].

3.3. **Effect of Message Length on Signing Time.** Table 3.3 presents the signing time as a function of message length (32 bytes, 1 KB, 16 KB). All three schemes exhibit only modest increases in signing cost as the message grows. This behavior is theoretically expected because post-quantum signature schemes adopt a **hash-then-sign** paradigm: the message is first compressed using a hash function (e.g., SHAKE256), and the resulting digest—not the full message—is incorporated into the lattice-based signing procedure [8]. As a result, the

TABLE 3.3. Average signing time (ms/op) as a function of message length

Algorithm	32 B	1 KB	16 KB
ML-DSA-44	0.08019	0.08534	0.13618
ML-DSA-65	0.12638	0.12718	0.17833
Falcon-512	0.22014	0.22285	0.26021

dominant computational cost is the internal lattice arithmetic (polynomial multiplications, NTT-based transforms, sampling steps), rather than message processing. Our results empirically confirm prior claims that hashing contributes only a negligible fraction of the total runtime [8, 7].

3.4. **Comparison with Existing Benchmark Literature.** Compared with SUPERCOP and PQClean results, which often rely on AVX2-optimized or handcrafted assembly implementations [9, 10, 12], the runtimes reported here are notably slower. This discrepancy is expected because our experiments deliberately use reference implementations, which trade speed for portability and clarity.

Nevertheless, the relative ordering among schemes—ML-DSA faster than Falcon for signing and key generation, Falcon significantly smaller in memory footprint—remains consistent with the performance trends documented in earlier PQC studies [5, 6].

These results therefore provide a clean, reproducible baseline that complements the highly optimized benchmarking performed in prior work, while removing architectural dependencies that often obscure true algorithmic cost.

4. Results and Discussion

The empirical findings presented in Section 3 reveal distinct computational profiles for the three standardized lattice-based signature schemes examined in this study. The observed trends are consistent with the theoretical structure of the algorithms as well as previously published benchmark results [9, 10, 5, 6].

4.1. **Comparative Performance Interpretation.** ML-DSA-44 demonstrates the fastest performance in both key generation and signing. This is expected due to its relatively small parameter set and the efficiency of the Fiat–Shamir-with-abort paradigm, which relies primarily on structured polynomial multiplications and lightweight rejection sampling. As the security level increases, ML-DSA-65 incurs higher computational cost, but the increase remains moderate. This aligns with analytic observations that the module dimension and polynomial degree scale in a controlled manner within the ML-DSA parameter hierarchy [5].

Falcon-512, by contrast, exhibits a markedly different computational pattern. Although it achieves significantly smaller public keys, secret keys, and signatures—an asset particularly valuable in constrained environments—its key generation time is nearly two orders of magnitude slower than that of ML-DSA. This gap is well documented in the NIST PQC literature and arises from Falcon's reliance on Fourier-based Gaussian sampling, which requires numerically stable floating-point operations and careful error control [6, 7]. These operations are both computationally dense and highly sensitive to microarchitectural details, which explains the large performance disparity even on modern processors equipped with AVX2 support [12].

Verification performance is more uniform across schemes. ML-DSA variants maintain a slight advantage, but the differences remain small, consistent with prior SUPERCOP and PQClean evaluations [9, 10]. This suggests that verification cost is not a primary bottleneck for any of the standardized schemes, even in high-throughput environments such as certificate validation pipelines or TLS handshake scenarios.

4.2. **Impact of Message Length: Hashing vs. Lattice Computation.** A key observation from Table 3.3 is that signing time increases only minimally as the message length grows from 32 bytes to 16 KB. This behavior is theoretically expected: all NIST-standardized PQC signature schemes adopt a hash-then-sign construction where the raw message is first compressed into a fixed-length digest before entering the lattice-based signing procedure.

Since the cost of hashing (e.g., SHAKE256) is negligible compared with lattice operations such as NTT-based polynomial multiplication or Gaussian sampling, the total signing time is effectively dominated by the latter [8]. Our results empirically confirm this theoretical expectation and reinforce the idea that signature performance in PQC systems is largely independent of message size, simplifying performance modeling for real-world deployments.

4.3. **Comparison with Optimized Implementations.** It is important to emphasize that the results reported here differ substantially from those obtained using optimized implementations such as the AVX2-enhanced PQClean backends or the handcrafted SUPERCOP assembly routines [9, 10, 12]. In optimized environments, Falcon often closes much of the performance gap with ML-DSA, particularly in signing and verification, while still lagging

in key generation. In contrast, our reference-only measurements provide a platform-neutral baseline that isolates the inherent computational cost of each scheme independent of hardware capabilities.

This distinction highlights a broader methodological point: optimized benchmarks answer the question *"What is the maximum attainable performance on a specific architecture?"*, while reference benchmarks answer *"What is the intrinsic cost of the algorithm itself?"*. Both perspectives are essential to understanding real-world PQC deployments.

4.4. **Implications for Deployment and System Design.** From an applied cryptography perspective, the results have direct implications for the design of PQC-enabled systems:

- **High-throughput environments:** ML-DSA-44 and ML-DSA-65 are strong candidates for systems that require frequent key generation or bulk signing, such as certificate authorities, distributed authentication services, and blockchain-based consensus networks.
- **Bandwidth- or memory-constrained environments:** Falcon-512 remains attractive for applications where key or signature size is critical—such as embedded IoT devices, mobile systems, or satellite communication—despite its slower key generation.
- **Hybrid cryptographic protocols:** These findings support hybrid PQC–classical deployments where Falcon may be combined with classical signatures for compact transmission, while ML-DSA may be preferred for server-side signing workloads.

Overall, the results reinforce a complementary relationship between ML-DSA and Falcon, consistent with NIST's decision to standardize both families. Rather than identifying a single "best" post-quantum signature scheme, the empirical evidence suggests a landscape in which algorithm choice is highly dependent on application requirements and resource constraints.

5. Conclusion

This work presented a reproducible performance evaluation of the standardized lattice-based post-quantum signature schemes ML-DSA-44, ML-DSA-65, and Falcon-512 using their reference implementations. The results show that ML-DSA variants provide the fastest key generation and signing performance, while Falcon-512 offers significantly smaller public keys, secret keys, and signatures at the cost of slower key generation. Verification times remain comparable across all schemes.

The experiments further indicate that signing time depends only weakly on message length, reflecting the dominance of lattice operations over hashing in overall computation. These findings highlight the practical trade-offs between speed and parameter size and demonstrate that the choice of signature scheme should be guided by the specific requirements of the target application.

Future work may focus on optimized implementations, alternative hardware platforms, and the behavior of these schemes in memory-constrained or side-channel-resistant settings.

References

[1] Regev, O. (2009). On lattices, learning with errors, random linear codes, and cryptography. Journal of the ACM (JACM), 56(6), 1-40.

[2] National Institute of Standards and Technology (NIST). (2015) FIPS 202: SHA-3 Standard: Permutation-Based Hash and Extendable-Output Functions. Federal Information Processing Standards Publication 202, https://doi.org/10.6028/NIST.FIPS.202.

[3] Peikert, C. (2016). A decade of lattice cryptography. Foundations and trends in theoretical computer science, 10(4), 283-424.

[4] Alagic, G., Alagic, G., Apon, D., Cooper, D., Dang, Q., Dang, T., ... & Smith-Tone, D. (2022). Status report on the third round of the NIST post-quantum cryptography standardization process.

[5] Ducas, L., Lepoint, T., Lyubashevsky, V., Schwabe, P., Seiler, G., & Stehlé, D. (2018). Crystals–dilithium: Digital signatures from module lattices.

[6] Fouque, P. A., Hoffstein, J., Kirchner, P., Lyubashevsky, V., Pornin, T., Prest, T., ... & Zhang, Z. (2018). Falcon: Fast-Fourier lattice-based compact signatures over NTRU. Submission to the NIST's post-quantum cryptography standardization process, 36(5), 1-75.

[7] Prest, T. (2015). Gaussian sampling in lattice-based cryptography (Doctoral dissertation, Ecole normale supérieure-ENS PARIS).

[8] Katz, J., & Lindell, Y. (2007). Introduction to modern cryptography: principles and protocols. Chapman and hall/CRC.

[9] Bernstein, D. J., & Lange, T. (2009). Supercop: System for unified performance evaluation related to cryptographic operations and primitives.(2009).

[10] Kannwischer, M. J., Schwabe, P., Stebila, D., & Wiggers, T. (2022, June). Improving software quality in cryptography standardization projects. In 2022 IEEE European Symposium on Security and Privacy Workshops (EuroS&PW) (pp. 19-30). IEEE.

[11] Howe, J., & Westerbaan, B. (2023, July). Benchmarking and analysing the NIST PQC lattice-based signature schemes standards on the ARM Cortex M7. In International Conference on Cryptology in Africa (pp. 442-462). Cham: Springer Nature Switzerland.

[12] Lei, D., He, D., Peng, C., Luo, M., Liu, Z., & Huang, X. (2023). Faster implementation of ideal lattice-based cryptography using avx512. ACM Transactions on Embedded Computing Systems, 22(5), 1-18.

(M. Karatay) Fenerbahçe University, İstanbul, Türkiye

CALCULATION

Volume ***2****, Issue* ***1****, 2026, Pages:****34–47***

E-ISSN: 3062–2107

www.simadp.com/calculation

MULTIPLICATIVE LEBESGUE SPACES

ERDEM TOKSOY *

Abstract. This study introduces Lebesgue spaces of multiplicative functions defined from the set of real numbers to the set of geometric real numbers; it is demonstrated that these spaces constitute multiplicative normed spaces, and multiplicative versions of Minkowski's and Hölder's inequalities are established.

Keywords: Multiplicative Lebesgue spaces, Multiplicative Minkowski's inequality, Multiplicative Hölder's inequality.

2020 Mathematics Subject Classification: 11U10, 26D15.

1. Introduction and Preliminaries

The operations of addition and subtraction serve as the foundation for classical calculus, which Newton and Leibniz established. In their fundamental *Non-Newtonian Calculus*, Grossman and Katz [9] showed that an unlimited number of unique calculi exist, each offering a self-consistent mathematical framework. They presented the notion of "generators" (γ-generators), which are bijective functions that alter the arithmetic of the real line, thus establishing novel operations for addition, subtraction, multiplication, and division. Through modifications to the foundational field operations, Grossman and Katz formulated an extended theory in which the classical derivative and integral are simply specific instances within a wider framework. Among the diverse calculi introduced by Grossman and Katz, the geometric calculus, also known as multiplicative calculus, has attracted the greatest scholarly interest in recent literature owing to its efficacy in addressing problems characterized by exponential growth and decay.

A generator is a bijective function whose domain is the set of real numbers $\mathbb{R}$ and whose codomain is a subset of $\mathbb{R}$. Take any generator γ with a range $B \subseteq \mathbb{R}$ and $u, v \in \mathbb{R}$. As to γ-arithmetic, we denote the arithmetic whose realm is B and whose operations are described as follows:

Received: 2025.11.01 *Revised: 2025.12.28* *Accepted: 2025.12.30*

* Corresponding author

Erdem Toksoy ⋄ erdem.toksoy@omu.edu.tr ⋄ https://orcid.org/0000-0003-3597-6161

$$\begin{aligned}
\gamma\text{-addition} \ : \quad u \oplus v &= \ \gamma\left\{\gamma^{-1}(u) + \gamma^{-1}(v)\right\} \\
\gamma\text{-subtraction} \ : \quad u \ominus v &= \ \gamma\left\{\gamma^{-1}(u) - \gamma^{-1}(v)\right\} \\
\gamma\text{-multiplication} \ : \quad u \odot v &= \ \gamma\left\{\gamma^{-1}(u) \times \gamma^{-1}(v)\right\} \\
\gamma\text{-division} \ : \quad u \oslash v &= \ \gamma\left\{\gamma^{-1}(u) \div \gamma^{-1}(v)\right\}
\end{aligned}$$

Specifically, if the γ-generator is given as the identity function, such that $\gamma(u) = u$ for all $u \in \mathbb{R}$, it follows that $\gamma^{-1}(u) = u$. Consequently, γ-arithmetic reduces to the classical arithmetic.

$$\begin{aligned}
\gamma\text{-addition} \ : u \oplus v = \gamma\{z + w\} = z + w \quad &: \text{ classical addition} \\
\gamma\text{-subtraction} \ : u \ominus v = \gamma\{u - v\} = u - v \quad &: \text{ classical subtraction} \\
\gamma\text{-multiplication} \ : u \odot v = \gamma\{u \cdot v\} = u \cdot v \quad &: \text{ classic multiplication} \\
\gamma\text{-division} \ : u \oslash v = \gamma\{u \div v\} = u \div v \quad &: \text{ classical division}
\end{aligned}$$

Employing the exponential function exp as the γ-generator, such that $\gamma(u) = \exp(u)$ for all $u \in \mathbb{R}$, it follows that $\gamma^{-1}(u) = \ln u$. Consequently, γ-arithmetic corresponds to the geometric arithmetic.

$$\begin{aligned}
\gamma\text{-addition} \ : u \oplus v = \exp(\ln u + \ln v) = u \cdot v \quad &: \quad \text{geometric addition} \\
\gamma\text{-subtraction} \ : z \ominus w = \exp(\ln u - \ln v) = u \div v \quad &: \quad \text{geometric subtraction} \\
\gamma\text{-multiplication} \ : z \odot w = \exp(\ln u \cdot \ln v) = u^{\ln v} \quad &: \quad \text{geometric multiplication} \\
\gamma\text{-division} \ : z \oslash w = \exp(\ln u \div \ln v) = u^{\frac{1}{\ln v}} \quad &: \quad \text{geometric division}
\end{aligned}$$

As a generator, we select the exponential function exp, which maps from the real numbers to the set $\mathbb{R}(G)$, where $\mathbb{R}(G)$ is defined as the set of positive real numbers. The set $\mathbb{R}(G)$ is indicated by

$$\mathbb{R}(G) := \{\exp(u) : u \in \mathbb{R}\} := \mathbb{R}^+.$$

In this context, the geometric zero is defined as $\exp(0) = 1$, whereas the geometric one is represented by $\exp(1) = e$. Also, the multiplicative absolute value of a geometric real number u is given as

$$|u|_M = \exp|\ln(u)|.$$

In geometric arithmetic, considering the monotonically increasing functions exp and ln, it is demonstrated that the fundamental order $<$ (or $\leq$) within the real numbers $\mathbb{R}$ is maintained within this arithmetic system.

One can give the definition of the multiplicative metric space as it is presented in the work by [22]. Consider U is a non-empty set and d_M is a function from $U \times U$ to $\mathbb{R}^+(G) \cup \{1\}$, where the following axioms hold for all $u, v, w \in U$:

i. $d_M\ (u, v) = 1$ if and only if $u = v$,
ii. $d_M\ (u, v) = d_M\ (v, u)$,
iii. $d_M\ (u, w) \leq d_M\ (u, v)\, d_M\ (v, w)$.

The function d_M is defined as a multiplicative metric function, and also (U, d_M) is said to be a multiplicative metric space. Let U be a vector space in the multiplicative sense over

the field $\mathbb{R}(G)$. Assume that $\|.\|_M$ is a function from U to $\mathbb{R}(G)$, where the following axioms hold for all $u, v \in U$ and $c \in \mathbb{R}(G)$:

(1) $\|u\|_M = 1$ if and only if $u = 0_U$,
(2) $\|cu\|_M = |c|_M \|u\|_M$,
(3) $\|uv\|_M \leq \|u\|_M \|v\|_M$.

Hence, $(U, \|.\|_M)$ is said a multiplicative normed space [22]. Also, this multiplicative norm $\|.\|_M$ on U determines a multiplicative metric d_M on U such that

$$d_M\ (u, v) = \left\| \frac{u}{v} \right\|_M$$

for all $u, v \in U$. This metric is described as the multiplicative metric induced by the multiplicative norm.

Furthermore, the collection of equivalence classes of measurable functions h mapping real numbers to real numbers that satisfy the condition

$$\int_{\mathbb{R}} |h(x)|^p \, d\mu(x) < \infty$$

is denoted by the symbol $L^p_{\mathbb{R}}(\mathbb{R})$.

In non-Newtonian calculus, the arithmetic of the domain and value sets of functions is crucial. Special instances of non-Newtonian calculus are classified based on these arithmetics. When the generating function, which is in the domain, is defined as the identity function I and the generating function, which is in the range, is represented by the exponential function exp, geometric calculus is established. In geometric calculus, classical arithmetic is employed in the domain region of a function, whereas geometric arithmetic is utilized in its range region. In certain studies the term "multiplicative calculus" is employed in the literature in place of "geometric calculus." The term "multiplicative" is meaningful due to the fact that multiplication in geometric calculus accomplishes the role of addition in classical calculus. Stanley [21] further advanced the pedagogical comprehension of this calculus by contrasting the "arithmetic" character of classical calculus with the "geometric" nature of multiplicative operations. The essential characteristics of multiplicative calculus, including the derivative and integral for positive real-valued functions, are comprehensively analyzed in [2]. The multiplicative calculus for complex-valued functions is examined at length in references [24, 1, 3]. Afterward, the paper [22] addressed complex sequence spaces from the perspective of geometric calculus. Although most of the multiplicative calculus works mentioned above do not explicitly mention generator functions, it is evident that the derivative and integral definitions provided in these works are derivative and integral definitions for functions for which classical arithmetic is employed in the domain region and geometric arithmetic is used in the range region.

In the article [7], the Lebesgue measure of real numbers is considered in a non-Newtonian context. The investigation of non-Newtonian Lebesgue measure and non-Newtonian measurable sets has been extensively examined in references [16, 17, 18, 19]. Subsequently, the basic features of non-Newtonian Lebesgue spaces are examined in the paper [8]. The studies [14, 15], examine measurable sets of positive real numbers within the framework of multiplicative calculus.

The research conducted by [5] and [23] is cited for investigations pertaining to non-Newtonian sequence spaces. Specifically, non-Newtonian Lebesgue sequence spaces and their geometric characteristics are examined in [10]. Based on recent research, relevant publications, including [20, 6], address multiplicative Lebesgue sequence spaces and their characteristics.

Furthermore, the current literature includes investigations into integral operators within the framework of non-Newtonian calculus and its particular instance, multiplicative calculus [25, 11, 12, 4].

Finally, in accordance with the last section of [13] that is about abstract measure integration in the multiplicative sense, it is observed that certain results related to are established.

2. Lebesgue Spaces of Geometric Real-Valued Functions

This section introduces multiplicative Lebesgue spaces, a specific case of non-Newtonian Lebesgue spaces as defined in [8]. In [8], non-Newtonian calculus is applied to the domain and range of the functions within the specified space. In geometric calculus, classical arithmetic applies to the domain of the specified functions, whereas geometric arithmetic pertains to the range. Consequently, the standard Lebesgue measurable space $(\mathbb{R}, \Sigma, \mu)$ is utilized in the domain while defining multiplicative Lebesgue spaces. Furthermore, in order to define the concept of a function being multiplicative-measurable, we will use the generator function as the exp function in the definition provided in [8], as geometric arithmetic is employed in the range of the functions specified in multiplicative calculus.

To begin, we will define the multiplicative-characteristic function and the multiplicative-simple function by replacing the generator function with the exp function in the general definitions provided in [8].

Definition 2.1. *Let A be any subset of $\mathbb{R}$. Then, a multiplicative characteristic function χ_A^M is defined by*

$$\chi_A^M(x) = \begin{cases} e, & x \in A \\ 1, & x \notin A \end{cases}.$$

Also, a function ρ from $\mathbb{R}$ to $\mathbb{R}(G)$ is called multiplicative simple function that is denoted by

$$\rho = \exp\left(\sum_{j=1}^{k} \ln(a_j) \ln\left(\chi_{B_j}^M\right)\right)$$

for some $k \in \mathbb{N}$, such that $a_j \in \mathbb{R}(G)$ and $B_j \in \Sigma$ for all $j = 1, 2, \ldots k$. Therefore, the definition of the multiplicative integral of a multiplicative simple function ρ on A is as follows:

$$\int_{\mathbb{R}}^{M} \rho^{d\mu} = \exp\left(\sum_{j=1}^{k} \ln(a_j)\, \mu(B_j)\right).$$

Definition 2.2. *A function $g : \mathbb{R} \longrightarrow \mathbb{R}(G) \cup \{+\infty\}$ is said to be multiplicative measurable if,*

$$\{x \in \mathbb{R} |\ \ln(g(x)) > \ln(\gamma)\} \in \Sigma$$

for all $\gamma \in \mathbb{R}(G)$.

Lemma 2.1. *A function $g : \mathbb{R} \longrightarrow \mathbb{R}(G)$ is multiplicative measurable if and only if $\ln g$ is measurable.*

Proof. Let us take a multiplicative measurable function g. Then, we write

$$\{x \in \mathbb{R}| \ \ln(g(x)) > \ln(\gamma)\} \in \Sigma,$$

for all $\gamma \in \mathbb{R}(G)$. There exists a $\beta \in \mathbb{R}$ such that $\gamma = \exp(\beta)$, for each $\gamma \in \mathbb{R}(G)$. Then, we obtain

$$\{x \in \mathbb{R}| \ \ln(g(x)) > \ln(\gamma)\} = \{x \in \mathbb{R}| \ \ln(g(x)) > \beta\} \in \Sigma,$$

for all $\beta \in \mathbb{R}$. This means that the function $\ln g$ is measurable.

Now, let us take a measurable function $\ln g$. Therefore, we have

$$\{x \in \mathbb{R}| \ \ln(g(x)) > \beta\} \in \Sigma,$$

for all $\beta \in \mathbb{R}$. Similarly, given that for each $\beta \in \mathbb{R}$ there exists a $\gamma \in \mathbb{R}(G)$ such that $\ln(\gamma) = \beta$, the statement

$$\{x \in \mathbb{R}| \ \ln(g(x)) > \beta\} = \{x \in \mathbb{R}| \ \ln(g(x)) > \ln(\gamma)\} \in \Sigma$$

is stated as desired. This indicates that the function g possesses multiplicative measurability. □

Proposition 2.1. *Let g and h be multiplicative measurable functions and $c \in \mathbb{R}(G)$. Then the functions gh and $c^{\ln g} = g^{\ln c}$ are also multiplicative measurable functions.*

Proof. Let g and h be multiplicative measurable functions and $c \in \mathbb{R}(G)$. By Lemma 2.1, the functions $\ln g$ and $\ln h$ are measurable functions. Given that the sum of two measurable functions is measurable, the function

$$\ln g + \ln h = \ln(gh)$$

is, as a result, measurable. Applying Lemma 2.1 once more, we state that the function gh is a multiplicative measurable function.

Considering Lemma 2.1, in the case where the function g is a multiplicative measurable function, the function $\ln g$ is a measurable function. Given that the product of a measurable function and a constant is still measurable, the function obtained by multiplying the measurable function $\ln g$ by a constant $\ln c$, denoted as

$$\ln c \ln g = \ln g^{\ln c}$$

is likewise measurable. Employing Lemma 2.1 again, we can establish that the function $g^{\ln c}$ is a multiplicative measurable function. □

Definition 2.3. *One can define the multiplicative absolute value and the positive and negative components of a multiplicative function. Let g be a multiplicative measurable function from $\mathbb{R}$ to $\mathbb{R}(G)$. Therefore, the following can be expressed:*

$$|g(x)|_M = \exp|\ln(g(x))|,$$

$$g^+(x) = \max_M(g(x), 1) = \exp(\max(\ln g(x), \ln 1)) = \exp(\max(\ln g(x), 0))$$

and

$$\begin{aligned} g^{-}(x) &= \max_{M}\left(\frac{1}{g(x)},1\right)=\exp\left(\max\left(\ln\frac{1}{g(x)},\ln 1\right)\right) \\ &= \exp\left(\max\left(-\ln g(x),0\right)\right), \end{aligned}$$

for all $x\in\mathbb{R}$. *Consider a set* $B\subset\mathbb{R}(G)$. *Hence, the multiplicative supremum of this set is as follows:*

$$\sup_{M} B:=\exp\left(\sup_{b\in\ B}\left(\ln b\right)\right).$$

Assume that h *is a multiplicative measurable function from* $\mathbb{R}$ *to* $\mathbb{R}^{+}(G)\cup\{1\}$, *where* $\mathbb{R}^{+}(G)=\{u\in\mathbb{R}(G)|\ u>1\}$. *As a result, multiplicative integral of the function* h *is given to be*

$$\int_{\mathbb{R}}^{M} h^{d\mu}=\sup_{M}\left\{\int_{\mathbb{R}}^{M}\rho^{d\mu}\ \middle|\ \rho\ \textit{is multiplicative simple and}\ 1\leq\rho\leq h\right\}.$$

Proposition 2.2. *Let* g *be a multiplicative measurable function. Then, one can write*

$$g(x)=\frac{g^{+}(x)}{g^{-}(x)}\ \textit{and}\ \left|g(x)\right|_{M}=g^{+}(x)\,g^{-}(x),$$

for all $x\in\mathbb{R}$. *Also, the functions* g^{+}, g^{-} *and* $|g|_{M}$ *are multiplicative measurable functions.*

Proof. Let g be a multiplicative measurable function. Thus, we have

$$g(x)=\exp\left(h(x)\right),$$

where h is a function from $\mathbb{R}$ to $\mathbb{R}$. Therefore, we determine

$$g=\exp(h)=\exp\left(h^{+}-h^{-}\right)$$

such that h^{+} and h^{-} are the positive and negative parts of the function h, respectively. Hence, we obtain

$$\begin{aligned} g(x) &= \exp\left(h^{+}(x)-h^{-}(x)\right) \\ &= \exp\left(\max\left(h(x),0\right)-\max\left(-h(x),0\right)\right) \\ &= \exp\left(\max\left(\ln g(x),0\right)-\max\left(-\ln g(x),0\right)\right) \\ &= \frac{\exp\left(\max\left(\ln g(x),0\right)\right)}{\exp\left(\max\left(-\ln g(x),0\right)\right)}=\frac{g^{+}(x)}{g^{-}(x)}, \end{aligned}$$

for all $x\in\mathbb{R}$. Initially, let us consider the positive and negative components of the function $\ln g$ as $(\ln g)^{+}$and $(\ln g)^{-}$, respectively. In this context, employing the relation

$$\left|\ln(g)\right|=(\ln g)^{+}+(\ln g)^{-}$$

results in

$$\begin{aligned} \left|g(x)\right|_{M} &= \exp\left|\ln\left(g(x)\right)\right| \\ &= \exp\left((\ln g)^{+}(x)+(\ln g)^{-}(x)\right) \\ &= \exp\left((\ln g)^{+}(x)\right)\exp\left((\ln g)^{-}(x)\right) \\ &= \exp\left(\max\left(\ln g(x),0\right)\right)\exp\left(\max\left(-\ln g(x),0\right)\right) \\ &= g^{+}(x)\,g^{-}(x), \end{aligned} \tag{2.1}$$

for all $x \in \mathbb{R}$. Let us now examine the multiplicative measurability of these functions. We have

$$g^{+}(x) = \exp\left(\max\left(\ln g(x), 0\right)\right) = \exp\left(\left(\ln g\right)^{+}(x)\right),$$

and

$$g^{-}(x) = \exp\left(\max\left(-\ln g(x), 0\right)\right) = \exp\left(\left(\ln g\right)^{-}(x)\right),$$

for all $x \in \mathbb{R}$. By Lemma 2.1, it is known that the function $\ln g$ is a measurable function. Given that the positive and negative components of a measurable function $\ln g$ are also measurable, the functions $(\ln g)^{+}$ and $(\ln g)^{-}$ are measurable. Consequently, by Lemma 2.1, the functions

$$g^{+} = \exp\left(\left(\ln g\right)^{+}\right)$$

and

$$g^{-} = \exp\left(\left(\ln g\right)^{-}\right)$$

are multiplicatively measurable. If the product of two multiplicative measurable functions, as delineated in Proposition 2.1, is likewise multiplicative measurable, then the function $|g|_{M}$, as characterized in equation (2.1), is multiplicative measurable. □

Definition 2.4. *Let g be a multiplicative measurable function. If*

$$\int_{\mathbb{R}}^{M} \left(|g(x)|_{M}\right)^{d\mu(x)} < \infty \tag{2.2}$$

holds, then the function g is said to be multiplicative integrable function. Therefore, multiplicative integral of the function g is given as

$$\int_{\mathbb{R}}^{M} g^{d\mu} = \frac{\int_{\mathbb{R}}^{M} \left(g^{+}\right)^{d\mu}}{\int_{\mathbb{R}}^{M} \left(g^{-}\right)^{d\mu}}.$$

Remark 2.1. *Given that both Riemann and Lebesgue integral calculus produce identical outcomes in $\mathbb{R}$ (excluding cases where functions are not Riemann-integrable but are Lebesgue-integrable), the following integration method presented by* [2] *is applicable for computing the Lebesgue integral. Let g be multiplicative measurable function and (2.2) holds, then*

$$\int_{\mathbb{R}}^{M} g(x)^{d\mu(x)} = \exp\left(\int_{\mathbb{R}} \ln g(x)\, d\mu(x)\right). \tag{2.3}$$

Now, we will provide a lemma that demonstrates that the inequality in (2.2) also guarantees that the integral in (2.3) has a finite value.

Lemma 2.2. *Let g be multiplicative measurable function. Then we get*

$$\left|\int_{\mathbb{R}}^{M} g(x)^{d\mu(x)}\right|_{M} \leq \int_{\mathbb{R}}^{M} \left(|g(x)|_{M}\right)^{d\mu(x)}.$$

Proof. Let g be a multiplicative measurable function. By Proposition 2.2 the function $|g|_M$ is also a multiplicative measurable function. Hence, we have

$$\begin{aligned}
\left|\int_{\mathbb{R}}^{M} g(x)^{d\mu(x)}\right|_M &= \left|\exp\left(\int_{\mathbb{R}} \ln g(x)\, d\mu(x)\right)\right|_M \\
&= \exp\left|\ln\left(\exp\left(\int_{\mathbb{R}} \ln g(x)\, d\mu(x)\right)\right)\right| \\
&= \exp\left|\int_{\mathbb{R}} \ln g(x)\, d\mu(x)\right| \\
&\leq \exp\int_{\mathbb{R}} |\ln g(x)|\, d\mu(x) \\
&= \exp\left(\int_{\mathbb{R}} \ln\left(\exp\left(|\ln g(x)|\right)\right) d\mu(x)\right) \\
&= \int_{\mathbb{R}}^{M} \left(\exp\left(|\ln g(x)|\right)\right)^{d\mu(x)} = \int_{\mathbb{R}}^{M} \left(|g(x)|_M\right)^{d\mu(x)}. \qquad (2.4)
\end{aligned}$$

This is the desired result. Also, combining (2.2) and (2.4) we obtain

$$\left|\int_{\mathbb{R}}^{M} g(x)^{d\mu(x)}\right|_M < \infty.$$

In conclusion, the integral in (2.3) has a finite value if the inequality (2.2) is valid. □

The set of multiplicative integrable functions from $\mathbb{R}$ to $\mathbb{R}(G)$ is denoted as $\mathcal{L}_{\mathbb{R}(G)}(\mathbb{R})$.

Theorem 2.1. *The following statements are valid.*

i. Let g be a function from $\mathbb{R}$ to $\mathbb{R}(G)$. If $g(x) = 1$ almost everywhere, then $g \in \mathcal{L}_{\mathbb{R}(G)}(\mathbb{R})$ and $\int_{\mathbb{R}}^{M} g(x)^{d\mu(x)} = 1$.

ii. Let $c \in \mathbb{R}(G)$ and $g, h \in \mathcal{L}_{\mathbb{R}(G)}(\mathbb{R})$. Then the functions gh and $c^{\ln g} = g^{\ln c}$ belong to $\mathcal{L}_{\mathbb{R}(G)}(\mathbb{R})$ and

$$\int_{\mathbb{R}}^{M} g(x)\, h(x)^{d\mu(x)} = \int_{\mathbb{R}}^{M} g(x)^{d\mu(x)} \int_{\mathbb{R}}^{M} h(x)^{d\mu(x)}, \qquad (2.5)$$

$$\int_{\mathbb{R}}^{M} \left(c^{\ln g(x)}\right)^{d\mu(x)} = c^{\ln\left(\int_{\mathbb{R}}^{M} g(x)^{d\mu(x)}\right)}. \qquad (2.6)$$

Additionally, through the utilization of these two operators gh and $c^{\ln g} = g^{\ln c}$, the set $\mathcal{L}_{\mathbb{R}(G)}(\mathbb{R})$ is a vector space in the multiplicative sense.

Proof.

i. Let g be a function from $\mathbb{R}$ to $\mathbb{R}(G)$, where $g(x) = 1$ almost everywhere. The multiplicative measurability of the constant function g is similar to the known measurability in $\mathbb{R}$. Also, we have

$$\int_{\mathbb{R}}^{M} \left(|g(x)|_M\right)^{d\mu(x)} = \exp \int_{\mathbb{R}} |\ln g(x)| \, d\mu(x) = \exp \int_{\mathbb{R}} 0 d\mu(x) = 1 < \infty$$

and

$$\int_{\mathbb{R}}^{M} \left(|g(x)|_M\right)^{d\mu(x)} = \exp \int_{\mathbb{R}} |\ln g(x)| \, d\mu(x) = \exp \int_{\mathbb{R}} 0 d\mu(x) = 1.$$

This means that $g \in \mathcal{L}_{\mathbb{R}(G)}(\mathbb{R})$.

ii. Let $c \in \mathbb{R}(G)$ and $g, h \in \mathcal{L}_{\mathbb{R}(G)}(\mathbb{R})$. Initially, we indicate that gh constitutes a multiplicative measurable function, as established by Proposition 2.1. Also, we write

$$\begin{aligned}
\int_{\mathbb{R}}^{M} \left(g(x) h(x)\right)^{d\mu(x)} &= \exp \int_{\mathbb{R}} \ln \left(g(x) h(x)\right) d\mu(x) \\
&= \exp \int_{\mathbb{R}} \left(\ln g(x) + \ln h(x)\right) d\mu(x) \\
&= \exp \left(\int_{\mathbb{R}} \ln g(x) \, d\mu(x) + \int_{\mathbb{R}} \ln h(x) \, d\mu(x) \right) \\
&= \exp \left(\int_{\mathbb{R}} \ln g(x) \, d\mu(x) \right) \exp \left(\int_{\mathbb{R}} \ln h(x) \, d\mu(x) \right) \\
&= \int_{\mathbb{R}}^{M} g(x)^{d\mu(x)} \int_{\mathbb{R}}^{M} h(x)^{d\mu(x)}.
\end{aligned}$$

This indicates that $gh \in \mathcal{L}_{\mathbb{R}(G)}(\mathbb{R})$. Now, we will demonstrate that $c^{\ln g} = g^{\ln c}$ belongs to $\mathcal{L}_{\mathbb{R}(G)}(\mathbb{R})$. Considering Proposition 2.1, we confirm that the function

$c^{\ln g} = g^{\ln c}$ is a multiplicative measurable function. Furthermore, we write

$$\begin{aligned}
\int_{\mathbb{R}}^{M} \left(c^{\ln g(x)}\right)^{d\mu(x)} &= \exp \int_{\mathbb{R}} \ln\left(c^{\ln g(x)}\right) d\mu\left(x\right) \\
&= \exp \int_{\mathbb{R}} \ln g\left(x\right) \ln c \; d\mu\left(x\right) \\
&= \exp\left(\ln c \int_{\mathbb{R}} \ln g\left(x\right) d\mu\left(x\right)\right) \\
&= \left(\exp \int_{\mathbb{R}} \ln g\left(x\right) d\mu\left(x\right)\right)^{\ln c} \\
&= \left(\int_{\mathbb{R}}^{M} g\left(x\right)^{d\mu(x)}\right)^{\ln c} = c^{\ln\left(\int_{\mathbb{R}}^{M} g(x)^{d\mu(x)}\right)}.
\end{aligned}$$

It is straightforward to demonstrate that the set $\mathcal{L}_{\mathbb{R}(G)}\left(\mathbb{R}\right)$ is a vector space with operators gh and $c^{\ln g} = g^{\ln c}$.

□

Let $g, h \in \mathcal{L}_{\mathbb{R}(G)}\left(\mathbb{R}\right)$. Therefore, let us define a function $d_{\mathcal{L}_{\mathbb{R}(G)}}\left(g, h\right)$ as

$$d_{\mathcal{L}_{\mathbb{R}(G)}}\left(g, h\right) = \exp \int_{\mathbb{R}} \left|\ln \frac{g\left(x\right)}{h\left(x\right)}\right| d\mu\left(x\right).$$

This function fulfills conditions ii and iii of a multiplicative metric but raises an issue regarding the one component of condition i. Let us now examine this matter. Consider $d_{\mathcal{L}_{\mathbb{R}(G)}}\left(g, h\right) = 1$. Thus, we write

$$\int_{\mathbb{R}} \left|\ln \frac{g\left(x\right)}{h\left(x\right)}\right| d\mu\left(x\right) = 0.$$

This means that $\ln \frac{g(x)}{h(x)} = 0$ almost everywhere. Thus, we get $g\left(x\right) = h\left(x\right)$ almost everywhere. Consequently, the space $L_{\mathbb{R}(G)}\left(\mathbb{R}\right)$, characterized as a collection of equivalence classes of functions that are almost everywhere equal and belong to $\mathcal{L}_{\mathbb{R}(G)}\left(\mathbb{R}\right)$, will solve the aforementioned issue present in the axioms of a multiplicative metric space.

Definition 2.5. *Let us define multiplicative Lebesgue spaces as follows. Consider*

$$\mathcal{L}^{p}_{\mathbb{R}(G)}\left(\mathbb{R}\right) = \left\{ h|\ \ h \text{ is multiplicative measurable and } \exp \int_{\mathbb{R}} \left|\ln h\left(x\right)\right|^{p} d\mu\left(x\right) < \infty \right\}$$

for $1 \leq p < \infty$. One can describe the spaces $L^{p}_{\mathbb{R}(G)}\left(\mathbb{R}\right)$, in which their elements consist of equivalence classes of functions that are equal almost everywhere and belong to $\mathcal{L}^{p}_{\mathbb{R}(G)}\left(\mathbb{R}\right)$.

Definition 2.6. *Let g be an $\mathbb{R}(G)$-valued multiplicative measurable function on $\mathbb{R}$. Then the function g is an essentially bounded on $\mathbb{R}$, if there exists a constant $B \in [1, \infty)$ such that*

$$\mu\left\{ x \in \mathbb{R}|\ \ \left|g\left(x\right)\right|_{M} > B \right\} = 0.$$

In other words, g is the essentially bounded on $\mathbb{R}$, if $|g(x)|_M \leq B$ almost everywhere on $\mathbb{R}$. We define the essential supremum of g as the multiplicative infimum of the essential bounds of g on $\mathbb{R}$, where the multiplicative infimum of a set $A \subset \mathbb{R}(G)$ is

$$\inf_M A := \exp\left(\inf_{a\in A}(\ln a)\right).$$

The following definition is given for the essential supremum of g:

$$ess\sup_M g = \inf_M \{B \in [1,\infty) | \ |g(x)|_M \leq B \text{ almost everywhere}\}.$$

As a result, the space $\mathcal{L}^\infty_{\mathbb{R}(G)}$ is described as following.

$$\mathcal{L}^\infty_{\mathbb{R}(G)}(\mathbb{R}) = \left\{ g| \ g \text{ is multiplicative measurable and } ess\sup_M g < \infty \right\}$$

One can describe the space $L^\infty_{\mathbb{R}(G)}(\mathbb{R})$, in which its elements consist of equivalence classes of functions that are equal almost everywhere and belong to $\mathcal{L}^\infty_{\mathbb{R}(G)}$.

Lemma 2.3. *Let $1 \leq p < \infty$. Then $g \in L^p_{\mathbb{R}(G)}(\mathbb{R})$ if and only if $\ln g \in L^p_{\mathbb{R}}(\mathbb{R})$.*

Proof. Initially, it is evident that the statements $f = h$ almost everywhere and $\ln f = \ln h$ almost everywhere are identical. Consider $1 \leq p < \infty$. Let us take $g \in L^p_{\mathbb{R}(G)}(\mathbb{R})$. Then, the function g is a multiplicative measurable function. By Lemma 2.1, the function $\ln g$ is a measurable function. Based on the definition of set $L^p_{\mathbb{R}(G)}(\mathbb{R})$, it follows that

$$\exp\left(\int_{\mathbb{R}} |\ln g(x)|^p \, d\mu(x)\right) < \infty \tag{2.7}$$

and so

$$\int_{\mathbb{R}} |\ln g(x)|^p \, d\mu(x) < \infty. \tag{2.8}$$

This means that $\ln g \in L^p_{\mathbb{R}}(\mathbb{R})$. Let $\ln g \in L^p_{\mathbb{R}}(\mathbb{R})$. Then, the function $\ln g$ is a measurable function. By Lemma 2.1, the function g is a multiplicative measurable function. According to the definition of the set $L^p_{\mathbb{R}}(\mathbb{R})$ and the inequality (2.8), the inequality (2.7) holds. This indicates that $g \in L^p_{\mathbb{R}(G)}(\mathbb{R})$. □

Theorem 2.2. *Consider $1 \leq p < \infty$. Let $c \in \mathbb{R}(G)$ and $g, h \in L^p_{\mathbb{R}(G)}(\mathbb{R})$. Then the set $L^p_{\mathbb{R}(G)}(\mathbb{R})$ is a vector space in the multiplicative sense with two operators given as gh and $c^{\ln g} = g^{\ln c}$.*

Proof. Consider $1 \leq p < \infty$. Let $c \in \mathbb{R}(G)$ and $g, h \in L^p_{\mathbb{R}(G)}(\mathbb{R})$. By Lemma 2.3, we have $\ln g, \ln h \in L^p_{\mathbb{R}}(\mathbb{R})$. Given that the space $L^p_{\mathbb{R}}(\mathbb{R})$ is a vector space,

$$\ln g + \ln h = \ln(gh)$$

is an element of the space $L^p_{\mathbb{R}}(\mathbb{R})$. Therefore, Lemma 2.3 implies that $gh \in L^p_{\mathbb{R}(G)}(\mathbb{R})$. Considering the scalar $\ln c$, due to the vector space structure of $L^p_{\mathbb{R}}(\mathbb{R})$, it follows that

$$\ln c \ln g = \ln g^{\ln c} \in L^p_{\mathbb{R}}(\mathbb{R}).$$

Consequently, Lemma 2.3 establishes that $g^{\ln c}$ belongs to $L^p_{\mathbb{R}(G)}(\mathbb{R})$. The remaining axioms defining a vector space in the multiplicative sense are readily apparent. □

Proposition 2.3. *Consider $1 \leq p < \infty$. Let us take $g \in L^p_{\mathbb{R}(G)}(\mathbb{R})$. Then one can give a function $\|.\|_{L^p_{\mathbb{R}(G)}}$ that is defined as*

$$\|g\|_{L^p_{\mathbb{R}(G)}} = \exp\left(\int_{\mathbb{R}} |\ln g(x)|^p \, d\mu(x)\right)^{\frac{1}{p}}.$$

Therefore, the space $\left(L^p_{\mathbb{R}(G)}(\mathbb{R}), \|.\|_{L^p_{\mathbb{R}(G)}}\right)$ is a multiplicative normed space.

Proof. Consider $1 \leq p < \infty$. Let us take $g \in L^p_{\mathbb{R}(G)}(\mathbb{R})$. By Lemma 2.3, we have $\ln g \in L^p_{\mathbb{R}}(\mathbb{R})$. It is established that the space $L^p_{\mathbb{R}}(\mathbb{R})$ constitutes a normed space endowed with the norm that is given as

$$\|h\|_{L^p_{\mathbb{R}}} = \left(\int_{\mathbb{R}} |h(x)|^p \, d\mu(x)\right)^{\frac{1}{p}}$$

for all $h \in L^p_{\mathbb{R}}(\mathbb{R})$. Therefore, we get

$$\|g\|_{L^p_{\mathbb{R}(G)}} = \exp\left(\|\ln g\|_{L^p_{\mathbb{R}}}\right), \tag{2.9}$$

for all $g \in L^p_{\mathbb{R}(G)}(\mathbb{R})$. By employing this final equality (2.9) along with the basic properties of the norm $\|.\|_{L^p_{\mathbb{R}}}$, we show that the function $\|.\|_{L^p_{\mathbb{R}(G)}}$ indeed constitutes a multiplicative norm. Let $g, h \in L^p_{\mathbb{R}(G)}(\mathbb{R})$ and $c \in \mathbb{R}(G)$.

i) If

$$\|g\|_{L^p_{\mathbb{R}(G)}} = \exp\left(\|\ln g\|_{L^p_{\mathbb{R}}}\right) = 1,$$

then

$$\|\ln g\|_{L^p_{\mathbb{R}}} = 0.$$

By the norm property of $\|.\|_{L^p_{\mathbb{R}}}$, we obtain $\ln g = 0$ almost everywhere and so $g = 1$ almost everywhere. If $g = 1$ almost everywhere, then

$$\|1\|_{L^p_{\mathbb{R}(G)}} = \exp\left(\|\ln 1\|_{L^p_{\mathbb{R}}}\right) = \exp\left(\|0\|_{L^p_{\mathbb{R}}}\right) = \exp(0) = 1.$$

ii)

$$\begin{aligned}
\left\|g^{\ln c}\right\|_{L^p_{\mathbb{R}(G)}} &= \exp\left(\left\|\ln\left(g^{\ln c}\right)\right\|_{L^p_{\mathbb{R}}}\right) = \exp\left(\|\ln c \ln g\|_{L^p_{\mathbb{R}}}\right) = \exp\left(|\ln c| \, \|\ln g\|_{L^p_{\mathbb{R}}}\right) \\
&= \left(\exp\left(\|\ln g\|_{L^p_{\mathbb{R}}}\right)\right)^{|\ln c|} = \left(\|g\|_{L^p_{\mathbb{R}(G)}}\right)^{\ln(\exp(|\ln c|))} = \left(\|g\|_{L^p_{\mathbb{R}(G)}}\right)^{\ln\left(|c|_M\right)}.
\end{aligned}$$

iii)

$$\begin{aligned}
\|gh\|_{L^p_{\mathbb{R}(G)}} &= \exp\left(\|\ln(gh)\|_{L^p_{\mathbb{R}}}\right) \\
&= \exp\left(\|\ln g + \ln h\|_{L^p_{\mathbb{R}}}\right) \\
&\leq \exp\left(\|\ln g\|_{L^p_{\mathbb{R}}} + \|\ln h\|_{L^p_{\mathbb{R}}}\right) \\
&= \exp\left(\|\ln g\|_{L^p_{\mathbb{R}}}\right) \exp\left(\|\ln h\|_{L^p_{\mathbb{R}}}\right) \\
&= \|g\|_{L^p_{\mathbb{R}(G)}} \|h\|_{L^p_{\mathbb{R}(G)}}.
\end{aligned} \tag{2.10}$$

This final equation (2.10) is referred to as the multiplicative form of Minkowski's inequality. □

Theorem 2.3 (Multiplicative Hölder's inequality)**.** *Consider* $1 \leq p, q < \infty$. *Let us take* $g \in L^p_{\mathbb{R}(G)}(\mathbb{R})$ *and* $h \in L^q_{\mathbb{R}(G)}(\mathbb{R})$, *where* $\frac{1}{p} + \frac{1}{q} = 1$. *Then* $g^{\ln h} = h^{\ln g} \in L^1_{\mathbb{R}(G)}(\mathbb{R})$ *and*

$$\left\| g^{\ln h} \right\|_{L^1_{\mathbb{R}(G)}} \leq \left(\|g\|_{L^p_{\mathbb{R}(G)}} \right)^{\ln\left(\|h\|_{L^q_{\mathbb{R}(G)}} \right)}.$$

Proof. Consider $1 \leq p, q < \infty$. Let us take $g \in L^p_{\mathbb{R}(G)}(\mathbb{R})$ and $h \in L^q_{\mathbb{R}(G)}(\mathbb{R})$, where $\frac{1}{p} + \frac{1}{q} = 1$. By using the equality (2.9) and Hölder's inequality, we determine

$$\begin{aligned}
\left\| g^{\ln h} \right\|_{L^1_{\mathbb{R}(G)}} &= \exp\left(\left\| \ln\left(g^{\ln h} \right) \right\|_{L^1_{\mathbb{R}}} \right) \\
&= \exp\left(\|\ln h \ln g\|_{L^1_{\mathbb{R}}} \right) \\
&\leq \exp\left(\|\ln g\|_{L^p_{\mathbb{R}}} \|\ln h\|_{L^q_{\mathbb{R}}} \right) \\
&= \left(\exp\left(\|\ln g\|_{L^p_{\mathbb{R}}} \right) \right)^{\|\ln h\|_{L^q_{\mathbb{R}}}} \\
&= \left(\exp\left(\|\ln g\|_{L^p_{\mathbb{R}}} \right) \right)^{\ln\left(\exp\left(\|\ln h\|_{L^q_{\mathbb{R}}} \right) \right)} \\
&= \left(\|g\|_{L^p_{\mathbb{R}(G)}} \right)^{\ln\left(\|h\|_{L^q_{\mathbb{R}(G)}} \right)}.
\end{aligned}$$

Since $g \in L^p_{\mathbb{R}(G)}(\mathbb{R})$ and $h \in L^q_{\mathbb{R}(G)}(\mathbb{R})$, the functions g and h are multiplicative measurable functions. According to Proposition 2.1, the function gh is a multiplicative measurable function. From the previous inequality, given that

$$\left\| g^{\ln h} \right\|_{L^1_{\mathbb{R}(G)}} \leq \left(\|g\|_{L^p_{\mathbb{R}(G)}} \right)^{\ln\left(\|h\|_{L^q_{\mathbb{R}(G)}} \right)} < \infty,$$

it follows that $g^{\ln h} = h^{\ln g} \in L^1_{\mathbb{R}(G)}(\mathbb{R})$. □

References

[1] Bashirov, A. E., & Riza, M. (2011). On complex multiplicative differentiation. TWMS Journal of Applied and Engineering Mathematics, 1(1), 75-85.

[2] Bashirov, A. E., Kurpınar, E. M. & Özyapıcı, A. (2008). Multiplicative calculus and its applications. Journal of Mathematical Analysis and Applications, 337(1), 36-48.

[3] Bashirov, A. E., & Norozpour, S. (2017). On complex multiplicative integration. TWMS Journal of Applied and Engineering Mathematics, 7(1), 82-93.

[4] Bhat, A. H., Majid, J., & Wani, I. A. (2019). Multiplicative Sumudu transform and its Applications. Emerging Tech. Innovative Res., 6(1), 579-589.

[5] Çakmak, A. F., & Başar, F. (2012). Some new results on sequence spaces with respect to non-Newtonian calculus. Journal of Inequalities and Applications, 2012(1), 1-12.

[6] Darweesh, A., Almalki, A., Al-Khaled, K., & Ayyash, A. (2024). A new view of spaces and their properties in the sense of non-Newtonian measure. PloS One, 19(12), 1-17.

[7] Duyar, C., & Sağır, B. (2017). Non-Newtonian comment of Lebesgue measure in real numbers. Journal of Mathematics, 2017, 1-5.

[8] Eryilmaz, İ. (2024). Non-Newtonian Lebesgue spaces with their basic features. Journal of Mathematical Extension, 18(7), 1-23.

[9] Grossman, M., & Katz, R. (1972). Non-Newtonian calculus: A self-contained, elementary exposition of the authors investigations. Massachussets, LeePress.

[10] Güngör, N. (2020). Some geometric properties of the non-Newtonian sequence spaces lp(N). Mathematica Slovaca, 70(3), 689-696.

[11] Güngör, N., & Dinc, N. (2024). Non-Newtonian Sumudu transform. Maejo International Journal of Science and Technology, 18(2), 130-145.

[12] Güngör, N., & Durmaz, H. (2020). Multiplicative Volterra integral equations and the relationship between multiplicative differential equations. Ikonion Journal of Mathematics, 2(2), 9-25.

[13] Moorthy, G. (2019). Applicable multiplicative calculus using multiplicative modulus function. Fundamental Journal of Mathematics and Applications, 2(2), 195-199.

[14] Oğur, O. (2024). On measurable sets in multiplicative calculus. Sağır, B. (Ed.), Special Subjects in Non-Newtonian Analysis (pp. 19-34). BIDGE Publication, ISBN:978-625-372-324-8.

[15] Oğur, O. (2024). A short note on measurable sets in multiplicative calculus. Duyar, C. (Ed.), Special Subjects in Non-Newtonian Analysis (pp. 81-96). BIDGE Publication, ISBN:978-625-372-324-8.

[16] Oğur, O., & Demir, S. (2019). On non-Newtonian measure for α-closed sets. New Trends in Mathematical Sciences, 7(2), 202-207.

[17] Oğur, O., & Demir, S. (2019). Newtonyen olmayan Lebesgue ölçüsü. Gümüşhane Üniversitesi Fen Bilimleri Dergisi, 10(1), 134-139.

[18] Oğur, O., & Güneş, Z. (2024). Newtonyen olmayan ölçülebilir kümeler üzerine bir not. Karadeniz Fen Bilimleri Dergisi, 14(1), 295-303.

[19] Oğur, O., & Gunes, Z. (2024). Vitali theorems in Non-Newtonian sense and non-Newtonian measurable functions. WSEAS Transactions on Mathematics, 23, 627-632.

[20] Sağır, B. & Eyüpoğlu, İ. (2022). Geometrik hesap tarzına göre Lebesgue dizi uzaylarının bazı geometrik özellikleri. Gümüşhane Üniversitesi Fen Bilimleri Dergisi, 12(2), 395-403.

[21] Stanley, D. (1999). A multiplicative calculus. PRIMUS, 9(4), 310-326.

[22] Turkmen, C., & Başar, F. (2012). Some basic results on the sets of sequences with geometric calculus. Communications Faculty of Sciences University of Ankara Series A1 Mathematics and Statistics, 61(2) , 17-34.

[23] Tekin, S., & Başar, F. (2013). Certain sequence spaces over the non-Newtonian complex field. In Abstract and Applied Analysis, 2013(1), 1-11.

[24] Uzer, A. (2010). Multiplicative type complex calculus as an alternative to the classical calculus. Computers & Mathematics with Applications, 60(10), 2725-2737.

[25] Yalcin, N., Celik, E., & Gokdogan, A. (2016). Multiplicative Laplace transform and its applications. Optik, 127(20), 9984-9995.

(E. Toksoy) Ondokuz Mayis University, Faculty of Science, Department of Mathematics, Samsun, Türkiye

CALCULATION

Volume **2**, *Issue* **1**, *2026, Pages:* **48–54**

E-ISSN: 3062–2107

www.simadp.com/calculation

SURFACES WITH IDEMPOTENT SHAPE OPERATOR MATRIX DEFINED ALONG A SURFACE CURVE

TUBA AKYILDIZ, SUDE ŞENYAZ, AND BAYRAM ŞAHIN *

Abstract. In this study, we investigate surfaces in differential geometry whose shape operator is idempotent. Such an algebraic constraint on the operator imposes strict geometric restrictions on the surface, particularly on its curvature functions. We classify surfaces according to the values of their Gaussian curvature, mean curvature, and principal curvatures when the shape operator matrix defined along a surface curve satisfies $S^2 = S$.

The results show that the idempotency condition leads to three distinct geometric cases depending on whether the geodesic torsion vanishes. These classifications provide insight into the structure of flat, minimal, elliptic, and umbilical surfaces.

Keywords: Shape operator, Idempotency, Principal curvature, Gaussian curvature, Mean curvature.

2020 Mathematics Subject Classification: Primary 53A05; Secondary 53A04, 53B20.

1. Introduction

Differential geometry studies the geometric and analytic properties of surfaces and curves. One of the central tools in this field is the shape operator, a symmetric linear transformation that encodes the bending behavior of a surface along different tangential directions.

A linear operator S is called idempotent if $S^2 = S$. Imposing this condition on the shape operator matrix defined along a surface curve produces strong geometric consequences and limits the possible curvature configurations of the surface. In this work, we classify surfaces based on the behavior of their curvature quantities under the idempotency condition.

The idempotency constraint $S^2 = S$ forces the normal curvatures and the geodesic torsion along the curve to take only specific values, which leads to three distinct geometric cases. As a result, we obtain a full local classification of such surfaces, when the geodesic torsion does not vanish, the surface must be flat with mean curvature $\frac{1}{2}$, while in the torsion-free case the surface is necessarily planar, spherical, or locally cylindrical depending on the pair

Received: 2025.10.14 *Revised: 2025.12.29* *Accepted: 2025.12.31*

* Corresponding author

Tuba Akyıldız ◇ tubaakyldz@gmail.com ◇ https://orcid.org/0009-0000-7107-6000

Sude Şenyaz ◇ senyaz.sude@gmail.com ◇ https://orcid.org/0009-0002-8300-0323

Bayram Şahin ◇ bayram.sahin@ege.edu.tr ◇ https://orcid.org/0000-0002-9372-1151

of normal curvatures. These findings illustrate how an algebraic condition on the shape operator imposes strong geometric sharpness, providing insight into the interplay between extrinsic curvature and operator theory on surfaces.

In this paper, all notions considered on a surface are assumed to be differentiable. Furthermore, the ring of differentiable functions on a surface is assumed to be an integral domain.

2. Preliminaries

In this section, we recall the basic concepts and formulas from the differential geometry of curves and surfaces that will be used throughout the paper. Let M be a regular surface with local parametrization $X(u, v)$ The coefficients of the first fundamental form $Edu^2 + 2Fdudv + Gdv^2$ are defined by

$$E = \langle X_u, X_u \rangle, \qquad F = \langle X_u, X_v \rangle, \qquad G = \langle X_v, X_v \rangle.$$

The first fundamental form measures lengths and angles on the surface.[1]

Let U be the unit normal vector field on M. The coefficients of the second fundamental form $Ldu^2 + 2Mdudv + Ndv^2$ are

$$L = \langle X_{uu}, U \rangle, \qquad M = \langle X_{uv}, U \rangle, \qquad N = \langle X_{vv}, U \rangle.$$

The second fundamental form captures how the surface bends in $\mathbb{R}^3$. [1] The normal curvature of γ at a point is defined by

$$k_n = \frac{Ldu^2 + 2M\, dudv + N\, dv^2}{E\, du2 + 2F\, dudv + G\, dv^2},$$

where E, F, G are the coefficients of the first fundamental form and L, M, N are the coefficients of the second fundamental form of the surface. [3] The geodesic torsion of the curve with respect to the surface is defined by [4]

$$\tau_g = \frac{(EM - FL)\,(u')^2 + (EN - GL)\,u'v' + (FN - GM)\,(v')^2}{\sqrt{EG - F^2}},$$

Let M be a regular oriented surface in $\mathbb{R}^3$ with unit normal vector field U. For a point $P \in M$, the tangent plane $T_P(M)$ consists of all tangent vectors of surface curves passing through P.[2]

The *shape operator* is the linear transformation

$$S_P : T_P(M) \longrightarrow T_P(M), \qquad S_P(X) = -D_X U,$$

where $D_X U$ denotes the directional derivative of the unit normal field U along the tangent vector X. Let S_P be the shape operator of the surface M at a point $P \in M$. The *Gaussian curvature* and *mean curvature* of M at P are defined by

$$K(P) = \det(S_P), \qquad H(P) = \frac{1}{2}\mathrm{trace}(S_P).$$

The eigenvalues of S_P are called the *principal curvatures* of M at P. [3]

Along a regular surface curve, the Darboux frame $\{T, V, U\}$ consists of:

$$T : \text{tangent vector}, \qquad U : \text{the unit normal vector of the surface}, \qquad V = U \times T.$$

The Darboux equations are

$$T' = k_g V + k_n U,$$
$$V' = -k_g T + \tau_g U,$$
$$U' = -k_n T - \tau_g V,$$

where k_g is the geodesic curvature and k_n is the normal curvature. [5]

Let M be a regular surface parametrized by $X(u, v)$ and $\beta(s) = X(u(s), v(s))$ a unit-speed curve lying on M. Let T, V, U denote the Darboux frame of β.

The *normal curvature* of M in the direction of V is

$$\kappa_n(V) = \frac{\lambda_1 (u')^2 + \lambda_2 u'v' + \lambda_3 (v')^2}{EG - F^2},$$

where along β,

$$\lambda_1 = F(FL - EM) + E(EN - FM),$$
$$\lambda_2 = F(GL - FM) + E(FN - GM),$$
$$\lambda_3 = G(GL - FM) + F(FN - GM).$$

Following the formulation given in [5], the matrix representation of S with respect to the Darboux frame $\{T, V\}$ along the surface curve is

$$S = \begin{pmatrix} k_n(T) & \tau_g \\ \tau_g & k_n(V) \end{pmatrix},$$

where $k_n(T)$ and $k_n(V)$ denote the normal curvatures and τ_g denotes the geodesic torsion. [4] The Gaussian curvature and mean curvature are given by

$$K = \det(S) = k_n(T) k_n(V) - \tau_g^2,$$
$$H = \frac{1}{2} \operatorname{trace}(S) = \frac{k_n(T) + k_n(V)}{2}.$$

The principal curvatures are

$$k_{1,2} = \frac{1}{2}(k_n(T) + k_n(V) \pm \sqrt{(k_n(T) - k_n(V))^2 + 4\tau_g^2})$$

A matrix $A \in \mathbb{R}^{n \times n}$ is called *idempotent* if

$$A^2 = A,$$

as defined in [6]. Such matrices represent linear transformations whose second application has no further effect; that is, $A(Ax) = Ax$ for all $x \in \mathbb{R}^n$. Idempotent matrices arise naturally in many areas of mathematics, including linear algebra, statistics, and differential geometry [6, 7, 8]

Idempotent matrices possess several well–known structural properties:

- Their eigenvalues can only be 0 or 1.
- The trace equals the rank: $\operatorname{tr}(A) = \operatorname{rank}(A)$
- If A is idempotent, then $I - A$ is also idempotent, and $A(I - A) = 0$.
- The transpose of an idempotent matrix is again idempotent.

Geometrically, idempotent matrices describe projections onto subspaces. For instance, the matrix

$$P = \begin{pmatrix} 1 & 0 \\ 0 & 0 \end{pmatrix}$$

represents the orthogonal projection onto the x–axis in $\mathbb{R}^2$ and satisfies $P^2 = P$. This interpretation is significant in our setting, since imposing the condition $S^2 = S$ on the shape operator forces the curvature directions to behave analogously to projection operators, which severely restricts the possible geometric configurations of the surface.

3. Main Results

In this section, we classify the local geometry of a surface along a curve under the assumption that the associated shape operator matrix is idempotent.

Theorem 3.1. *Let M be a surface and let S be the shape operator matrix defined along a surface curve with respect to the Darboux frame $\{T, V, U\}$. If S is idempotent, that is, $S^2 = S$, then the following hold:*

1) *If the geodesic torsion satisfies $\tau_g \neq 0$, then*

$$H = \tfrac{1}{2}, \qquad K = 0, \qquad k_1 = 1, \qquad k_2 = 0.$$

The surface is flat but not minimal, and it is non-umbilical.

2) *If $\tau_g = 0$, then the normal curvatures satisfy $k_n(T), k_n(V) \in \{0, 1\}$ and the following subcases arise:*
   A) $k_n(T) = k_n(V) = 0$
   B) $k_n(T) = k_n(V) = 1$
   C) $(k_n(T), k_n(V)) \in \{(1, 0), (0, 1)\}$*:*

Proof. Let the shape operator matrix along the surface curve be

$$S = \begin{pmatrix} k_n(T) & \tau_g \\ \tau_g & k_n(V) \end{pmatrix}.$$

The idempotency condition $S^2 = S$ yields

$$\begin{pmatrix} k_n(T)^2 + \tau_g^2 & k_n(T)\tau_g + \tau_g k_n(V) \\ \tau_g k_n(T) + k_n(V)\tau_g & \tau_g^2 + k_n(V)^2 \end{pmatrix} = \begin{pmatrix} k_n(T) & \tau_g \\ \tau_g & k_n(V) \end{pmatrix},$$

and therefore we have these equations

$$k_n(T)^2 + \tau_g^2 = k_n(T), \tag{3.1}$$

$$k_n(V)^2 + \tau_g^2 = k_n(V), \tag{3.2}$$

$$\tau_g \left(k_n(T) + k_n(V)\right) = \tau_g. \tag{3.3}$$

Case 1: $\tau_g \neq 0$ From (3.3) we obtain

$$k_n(T) + k_n(V) = 1.$$

Squaring this identity

$$\begin{aligned}\big(k_n(T)+k_n(V)\big)^2 &= k_n(T)^2+2k_n(T)k_n(V)+k_n(V)^2\\ &= 1 \quad \Rightarrow \quad k_n(T)^2+k_n(V)^2+2k_n(T)k_n(V)=1. \end{aligned} \tag{3.4}$$

Substituting $k_n(T)^2$ and $k_n(V)^2$ from (3.1)–(3.2) we obtain

$$\begin{aligned}(k_n(T)-\tau_g^2)+(k_n(V)-\tau_g^2)+2k_n(T)k_n(V)&=1\\ \Rightarrow \quad 2k_n(T)k_n(V)&=2\tau_g^2\\ \Rightarrow \quad k_n(T)k_n(V)&=\tau_g^2.\end{aligned}$$

Hence, the Gaussian curvature is

$$K=\det(S)=k_n(T)k_n(V)-\tau_g^2=0, \tag{3.5}$$

and the mean curvature is

$$H=\frac{k_n(T)+k_n(V)}{2}=\frac{1}{2}. \tag{3.6}$$

The principal curvatures are

$$k_1=1, \quad k_2=0. \tag{3.7}$$

Case 2: $\tau_g=0$**.** In this case, equations (3.1)–(3.2) become

$$k_n(T)^2-k_n(T)=0, \qquad k_n(V)^2-k_n(V)=0,$$

which imply

$$k_n(T),\, k_n(V)\in\{0,1\}.$$

Therefore, the possible geometric configurations are:

$k_n(T)=0,\ k_n(V)=0:$	$K=0,\ H=0;$	the surface is a plane or a planar patch,
$k_n(T)=1,\ k_n(V)=1:$	$K=1,\ H=1;$	the surface is elliptic and umbilical (e.g., unit sphere),
$k_n(T)\neq k_n(V):$	$K=0,\ H=\frac{1}{2};$	the surface is locally flat, non-minimal, and non-umbilical.

This completes the proof. □

4. Examples

In this section, we illustrate the cases of Theorem 3.1 by examining classical surfaces whose shape operator matrix becomes idempotent at certain points or along certain curves.

Example 4.1. ***Circular Cylinder.***

Consider the circular cylinder of radius r. Its principal curvatures are

$$k_1 = \frac{1}{r}, \qquad k_2 = 0.$$

The shape operator is idempotent if and only if its eigenvalues belong to $\{0, 1\}$, which requires

$$\frac{1}{r} = 1 \quad \Rightarrow \quad r = 1.$$

Thus, only the unit cylinder satisfies $S^2 = S$.

Along a general surface curve not aligned with principal directions, the geodesic torsion satisfies $\tau_g \neq 0$. Therefore, by Theorem 3.1 (Case 1),

$$K = 0, \qquad H = \frac{1}{2}, \qquad k_1 = 1, \qquad k_2 = 0.$$

Hence, the unit circular cylinder is a natural example of a surface whose idempotent shape operator corresponds to the nonzero–torsion case.

Example 4.2. ***Plane.*** *For a plane, all coefficients of the second fundamental form vanish:*

$$L = M = N = 0.$$

Thus, we have

$$k_n(T) = 0, \qquad k_n(V) = 0, \qquad \tau_g = 0.$$

The shape operator is the zero matrix, which trivially satisfies $S^2 = S$. This corresponds to Theorem 3.1 (Case 2A), giving

$$K = 0, \qquad H = 0, \qquad k_1 = k_2 = 0.$$

Example 4.3. ***Sphere.*** *For a sphere of radius R, both principal curvatures equal $1/R$:*

$$k_1 = k_2 = \frac{1}{R}.$$

Idempotency of the shape operator requires the eigenvalues to be 1, hence

$$\frac{1}{R} = 1 \quad \Rightarrow \quad R = 1.$$

Thus, the only sphere satisfying $S^2 = S$ is the one with a unit radius. Since all normal directions are principial, we have

$$k_n(T) = k_n(V) = 1, \qquad \tau_g = 0.$$

This corresponds to Theorem 3.1 (Case 2B), giving

$$K = 1, \qquad H = 1, \qquad k_1 = k_2 = 1.$$

Example 4.4. ***Parabolic Cylinder.***

Consider the parabolic cylinder $z = \frac{1}{2}x^2$. At the point $x = 0$, the principal curvatures of the parabolic cylinder satisfy $k_1 = 1$ and $k_2 = 0$. Hence, the eigenvalues of the shape operator belong to $\{0, 1\}$ at the point, and the idempotency condition requires the eigenvalues The idempotency condition $S^2 = S$ is satisfied only along the curve $\{x = 0\}$ The idempotency condition requires the eigenvalues of S to lie in $\{0, 1\}$. Thus,

$$\kappa(x) \in \{0, 1\}.$$

Since $\kappa(x) = 1$ only at $x = 0$, the idempotency condition is satisfied along the curve $\{x = 0\}$ on the surface.

At such a point we have

$$k_n(T) = 1, \qquad k_n(V) = 0, \qquad \tau_g = 0.$$

This corresponds to Theorem 3.1 (Case 2C), yielding

$$K = 0, \qquad H = \frac{1}{2}, \qquad k_1 = 1, \qquad k_2 = 0.$$

Thus, the parabolic cylinder provides an example of a surface for which the normal curvatures take different values in $\{0, 1\}$, and the shape operator is idempotent only along a specific curve.

5. Conclusion

In this work, we classified surfaces whose shape operator matrix defined along a surface curve is idempotent. The condition $S^2 = S$ imposes strong algebraic restrictions on the normal curvatures and geodesic torsion, resulting in three distinct geometric cases. These results connect an algebraic operator constraint with intrinsic and extrinsic geometry and contribute to the broader understanding of curvature-based surface classifications.

Acknowledgments. This study was supported by the TÜBİTAK 2209-A Research Project for Undergraduate Students.

References

[1] Şahin, B. (2022). *Diferansiyel geometri*. Palme Yayınevi.
[2] Şahin, B. (2012). *Manifoldların diferansiyel geometrisi*. Nobel Akademik Yayıncılık.
[3] Hacısalihoğlu, H. H. (1998). *Diferansiyel geometri*. Hacısalihoğlu Yayıncılık.
[4] Uyar Düldül, B., & Düldül, M. (2019). Shape operator via Darboux frame curvatures and its applications. *International Electronic Journal of Geometry, 12*(2), 182–187.
[5] Uyar Düldül, B., & Düldül, M. (2019). Extended Darboux frame curvatures of Frenet curves on parametric 3-surfaces. *Kuwait Journal of Science, 46*(1), 15–23.
[6] Nicholson, W. K. (1986). *Elementary linear algebra* (3rd ed.). Prindle, Weber & Schmidt.
[7] Harville, D. A. (1997). *Matrix algebra from a statistician's perspective*. Springer.
[8] Abadir, K. M., & Magnus, J. R. (2005). *Matrix algebra*. Cambridge University Press.

(T. Akyıldız, S. Şenyaz, B. Şahin) Department of Mathematics, Faculty of Science, Ege University, İzmir, Türkiye

VOLUME 2 ISSUE 1
E-ISSN: 3062-2107

January 2026
www.simadp.com/calculation

Contents